Spin and Orbital Angular Momenta of Electromagnetic Waves: A Preliminary Study

Wei E.I. Sha (沙威)

College of Information Science & Electronic Engineering
Zhejiang University, Hangzhou 310027, P. R. China

On leave from EEE Department, the University of Hong Kong

Email: weisha@zju.edu.cn
Website: http://www.isee.zju.edu.cn/weisha/

Contents

1. Theoretical Foundation

Momentum of Light

de Broglie hypothesis (wave-particle duality)

$$p = \hbar k = \hbar \frac{\omega}{c} = \frac{E}{c}$$

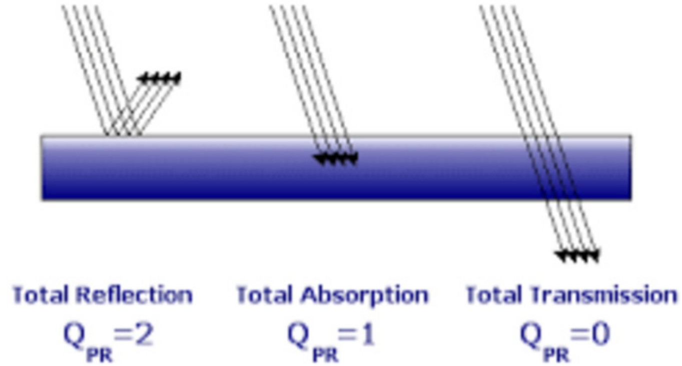

Linear momentum

$$\mathbf{P}^{em} = \frac{\int (\mathbf{E}\times\mathbf{H})\cdot ds\cdot dt}{c} = \frac{\int (\mathbf{E}\times\mathbf{H})\cdot ds\cdot dl}{c^2} = \frac{\int (\mathbf{E}\times\mathbf{H})dV}{c^2}$$

$$\boxed{\mathbf{P}^{em} = 1/c^2\cdot\int(\mathbf{E}\times\mathbf{H})dV = \varepsilon_0\int(\mathbf{E}\times\mathbf{B})dV}$$

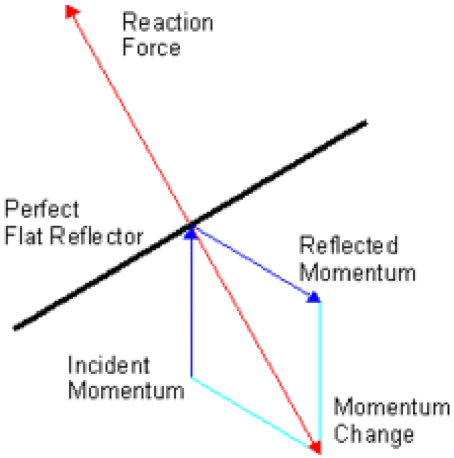

Splitting of linear momentum

$$\mathbf{P}^{em} = \varepsilon_0\int(\mathbf{E}_{\|}\times\mathbf{B})dV + \varepsilon_0\int(\mathbf{E}_{\perp}\times\mathbf{B})dV,\ \mathbf{E} = \underbrace{\mathbf{E}_{\|}}_{\text{longitudinal}} + \underbrace{\mathbf{E}_{\perp}}_{\text{transverse}}$$

$$\varepsilon_0\int(\mathbf{E}_{\|}\times\mathbf{B})dV \Rightarrow \varepsilon_0 L^3\sum_n \tilde{\mathbf{E}}_{\|,n}\times\tilde{\mathbf{B}}_n \qquad \nabla\cdot\mathbf{E} = \frac{\rho}{\varepsilon_0} \Rightarrow \tilde{\mathbf{E}}_{\|,n} = -\frac{i\mathbf{k}_n}{\varepsilon_0 k_n^2}\tilde{\rho}_n \qquad \nabla\times\mathbf{A} = \mathbf{B} \Rightarrow \tilde{\mathbf{B}}_n = i\tilde{\mathbf{k}}_n\times\tilde{\mathbf{A}}_n$$

$$\boxed{\varepsilon_0\int(\mathbf{E}_{\|}\times\mathbf{B})dV = \int dV\rho(\mathbf{r},t)\mathbf{A}(\mathbf{r},t) = \sum_n q_n(\mathbf{r}_n)\mathbf{A}(\mathbf{r}_n,t)}$$

related to field momentum
in quantum mechanism

Spin and Orbital Angular Momenta of Light

Time-averaged radiation momentum density

$$\mathbf{p}^{rad} = \frac{\varepsilon_0}{2}\mathrm{Re}(\mathbf{E}_\perp^* \times \mathbf{B}) = \frac{\varepsilon_0}{2}\mathrm{Re}(\mathbf{E}_\perp^* \times \mathbf{B}_\perp) \qquad \mathbf{l}^{rad} = \mathbf{r}\times\mathbf{p}^{rad}$$

angular momentum density

Splitting of time-averaged radiation momentum density

$$\frac{\varepsilon_0}{2}\mathrm{Re}(\mathbf{E}_\perp^* \times \mathbf{B}_\perp) = \underbrace{\frac{\varepsilon_0}{4\omega}\mathrm{Im}\left[\nabla\times(\mathbf{E}_\perp^*\times\mathbf{E}_\perp)\right]}_{\mathbf{p}^s} + \underbrace{\frac{\varepsilon_0}{2\omega}\mathrm{Im}\left[\mathbf{E}_\perp^*\cdot\nabla\mathbf{E}_\perp\right]}_{\mathbf{p}^o}$$

spin momentum density

orbital momentum density

Time-averaged spin and orbital angular momentum density

$$\boxed{\mathbf{l}^s = \mathbf{r}\times\mathbf{p}^s = \frac{\varepsilon_0}{2\omega}\mathrm{Im}\left[\mathbf{E}_\perp^*\times\mathbf{E}_\perp\right]} \qquad \boxed{\mathbf{l}^o = \mathbf{r}\times\mathbf{p}^o = \frac{\varepsilon_0}{2\omega}\mathrm{Im}\left[\mathbf{E}_\perp^*\cdot(\mathbf{r}\times\nabla)\mathbf{E}_\perp\right]}$$

spin angular momentum density

orbital angular momentum density

SAM and OAM — Photon versus Electron

OAM of photon

$$\mathbf{I}^o = \mathrm{Re}\left[\boldsymbol{\psi}^* \cdot \left(\mathbf{r}\times(-i\hbar\nabla)\right)\boldsymbol{\psi}\right]$$

$$\mathbf{I}^o = \mathrm{Re}\left\langle \boldsymbol{\psi} \,|\, \hat{\mathbf{L}} \,|\, \boldsymbol{\psi}\right\rangle, \quad \boldsymbol{\psi} = \sqrt{\frac{\varepsilon_0}{2\omega\hbar}}\mathbf{E} \rightarrow \hat{\mathbf{E}}$$

$$\hat{\mathbf{L}} = \mathbf{r}\times\hat{\mathbf{p}}, \quad \hat{\mathbf{p}} = -i\hbar\nabla$$

OAM of electron

$$\mathbf{I}^o = \left\langle \boldsymbol{\psi} \,|\, \hat{\mathbf{L}} \,|\, \boldsymbol{\psi}\right\rangle$$

$$\hat{\mathbf{L}} = \mathbf{r}\times\hat{\mathbf{p}}, \quad \hat{\mathbf{p}} = -i\hbar\nabla$$

SAM of photon

$$\mathbf{I}^s = \mathrm{Re}\left\langle \boldsymbol{\psi} \,|\, \hat{\mathbf{S}} \,|\, \boldsymbol{\psi}\right\rangle, \quad \boldsymbol{\psi} = \sqrt{\frac{\varepsilon_0}{2\omega\hbar}}\mathbf{E} \rightarrow \hat{\mathbf{E}}$$

$$\hat{\mathbf{S}}_x = -i\hbar\begin{pmatrix} 0 & 0 & 0 \\ 0 & 0 & 1 \\ 0 & -1 & 0 \end{pmatrix}, \quad \hat{\mathbf{S}}_y = -i\hbar\begin{pmatrix} 0 & 0 & -1 \\ 0 & 0 & 0 \\ 1 & 0 & 0 \end{pmatrix},$$

$$\hat{\mathbf{S}}_z = -i\hbar\begin{pmatrix} 0 & 1 & 0 \\ -1 & 0 & 0 \\ 0 & 0 & 0 \end{pmatrix}, \quad \left[\hat{\mathbf{S}}_x, \hat{\mathbf{S}}_y\right] = i\hbar\hat{\mathbf{S}}_z$$

SAM of electron

$$\mathbf{I}^s = \left\langle \boldsymbol{\psi} \,|\, \hat{\mathbf{S}} \,|\, \boldsymbol{\psi}\right\rangle$$

$$\hat{\mathbf{S}}_x = \frac{\hbar}{2}\begin{pmatrix} 0 & 1 \\ 1 & 0 \end{pmatrix}, \quad \hat{\mathbf{S}}_y = \frac{\hbar}{2}\begin{pmatrix} 0 & -i \\ i & 0 \end{pmatrix},$$

$$\hat{\mathbf{S}}_z = \frac{\hbar}{2}\begin{pmatrix} 1 & 0 \\ 0 & -1 \end{pmatrix}, \quad \left[\hat{\mathbf{S}}_x, \hat{\mathbf{S}}_y\right] = i\hbar\hat{\mathbf{S}}_z$$

Angular Momentum: A Simple Look

- Spin angular momentum (SAM): value S = 0, ±ħ
- Orbital angular momentum (OAM): value L = *l*ħ

Photon with SAM

S = 0

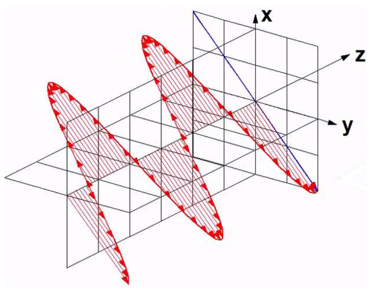

Linear Polarization

S = ±ħ

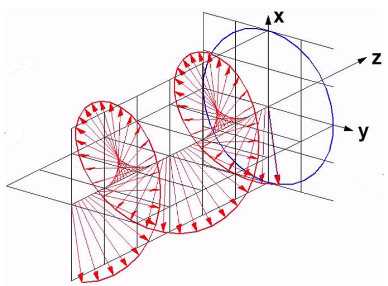

Circular Polarization

circularly polarized waves carry SAM!

Photon with OAM

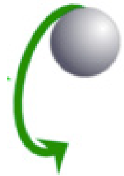

L = 0

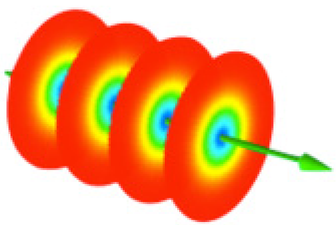

Plane Wavefront

L = ħ

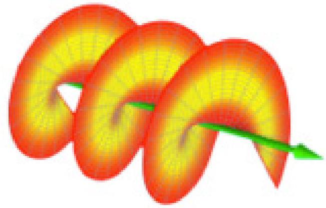

• • •

L = 2ħ

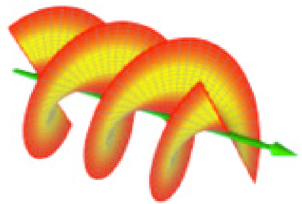

Twisted Wavefront

Vortex Beam Carrying OAM

➢ Laguerre-Gaussian Modes[1]

$$LG_{p\ell} = \sqrt{\frac{2p!}{\pi\,(p+|\ell|)!}}\frac{1}{w(z)}\left[\frac{r\sqrt{2}}{w(z)}\right]^{|\ell|}\exp\left[\frac{-r^2}{w^2(z)}\right]L_p^{|\ell|}\left(\frac{2r^2}{w^2(z)}\right)\boxed{\exp[i\ell\phi]}\exp\left[\frac{ik_0 r^2 z}{2(z^2+z_R^2)}\right]\exp\left[-i(2p+|\ell|+1)\tan^{-1}\left(\frac{z}{z_R}\right)\right]$$

Azimuthal phase dependence

ϕ , Azimuthal angle

Radial index

Azimuth index (Topological charge)

Phase singularity

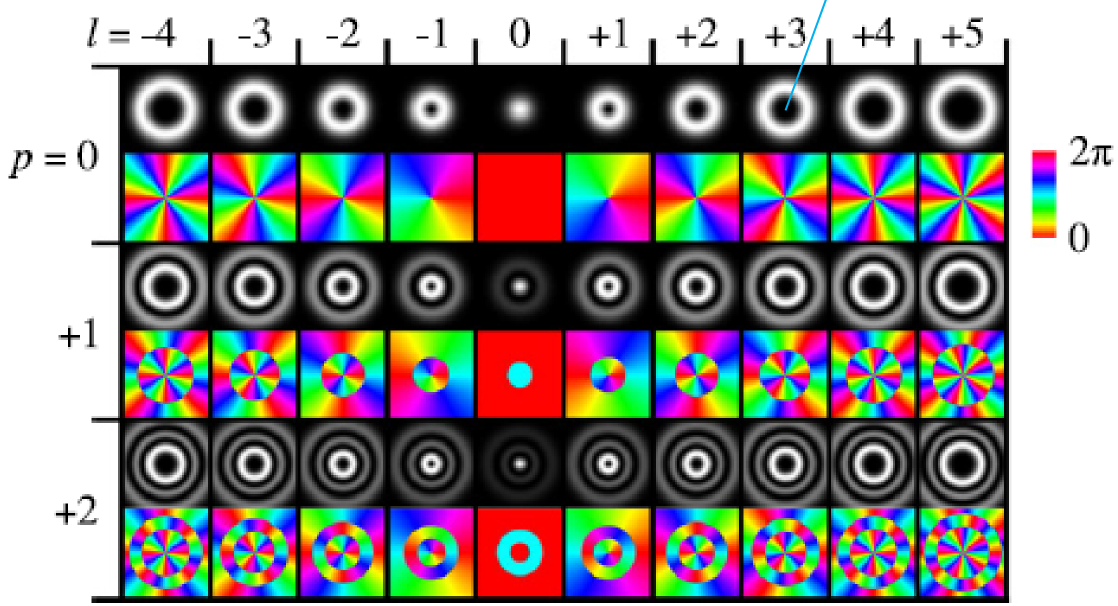

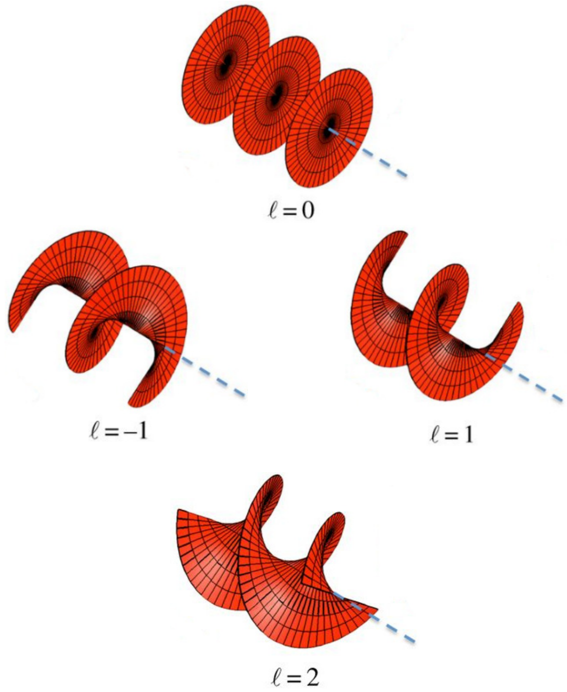

[1] A. M. Yao, and M. J. Padgett, "Orbital angular momentum: origins, behavior and applications," *Adv. Opt. Photonics*, vol. 3, no. 2, pp. 161-204, 2011.

2. Potential Applications

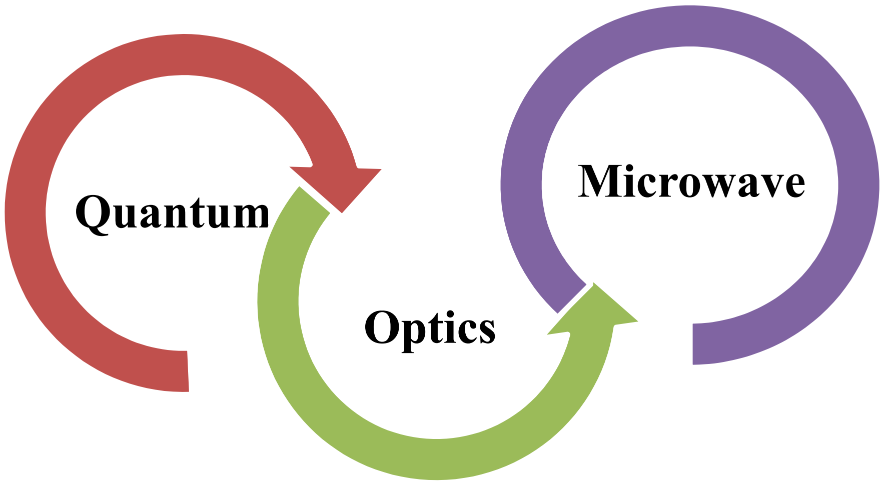

Communications

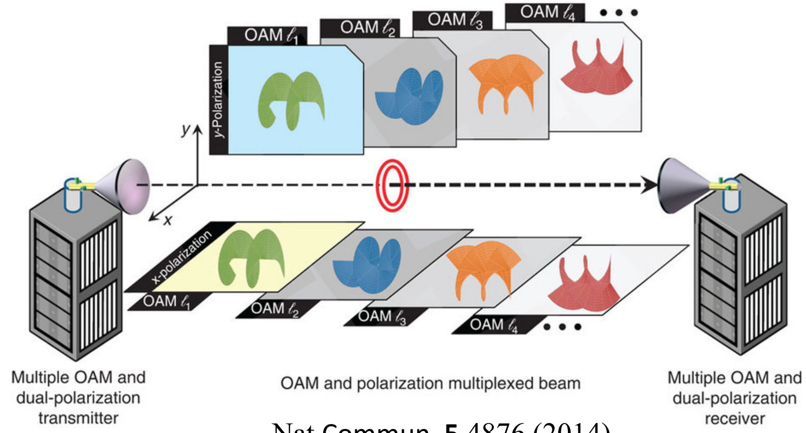

Nat Commun. **5** 4876 (2014)

Quantum Cryptography

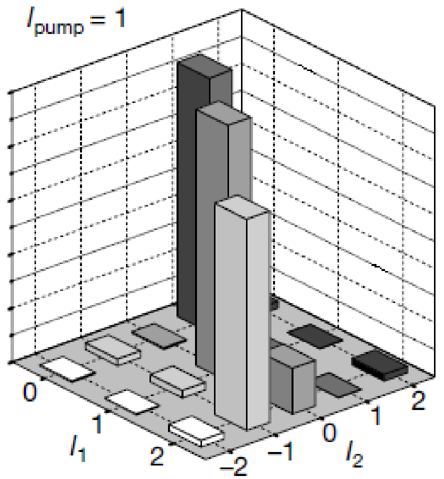

Nature **412** 19 (2001)

Optical Tweezer

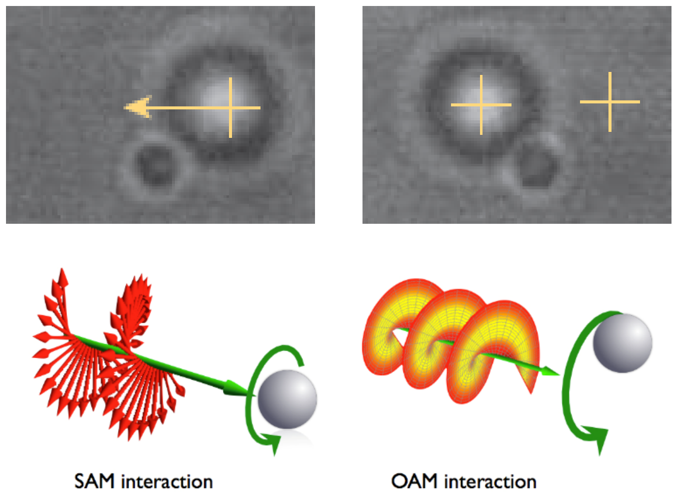

Nature **424** 21 (2003)

Molecular Detection

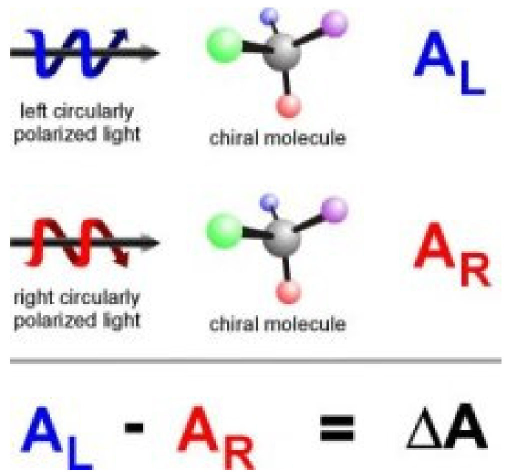

Nat Commun. **6** 7117 (2015)

3.1. Polarization Control by Using 3-D Chiral Structures

[1] M. L. N. Chen, L. J. Jiang, W. E. I. Sha, W. C. H. Choy, and T. Itoh, "Polarization control by using anisotropic 3-D chiral structures," *IEEE Trans. Antennas Propag.*, vol. 64, no. 11, pp. 4687-4694, Nov. 2016.

Introduction

- **Chiral medium**
  - composed of particles that <u>cannot be superimposed on their mirror images</u>
- **Examples**

3D chiral structure

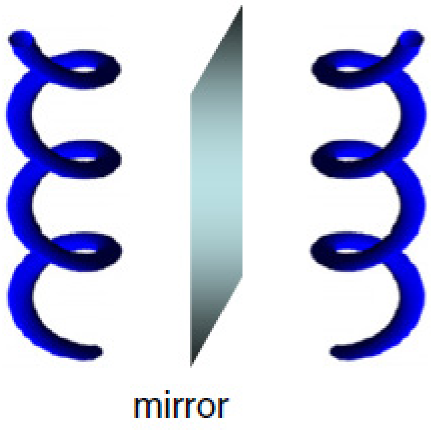

Planar chiral structure

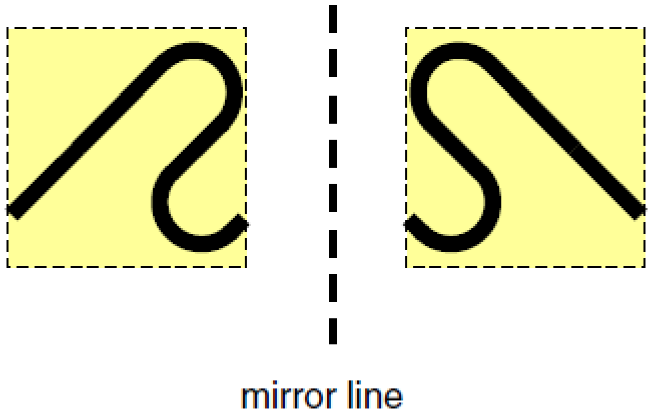

EM Property of Chiral Media

- **<u>BI</u>-isotropic and <u>BI</u>-anisotropic media**
  - Cross coupling between the electric and magnetic fields along the same direction

Constitutive relations

Bi-isotropic

$$\mathcal{D} = \epsilon \cdot \mathcal{E} + \boxed{\xi \cdot \mathcal{H}}$$

$$\mathcal{B} = \boxed{\zeta \cdot \mathcal{E}} + \mu \cdot \mathcal{H}$$

tensor form $\longrightarrow$

Bi-anisotropic

$$\mathbf{D} = \overline{\boldsymbol{\varepsilon}} \cdot \mathbf{E} + \overline{\boldsymbol{\xi}} \cdot \mathbf{H}$$

$$\mathbf{B} = \overline{\boldsymbol{\zeta}} \cdot \mathbf{E} + \overline{\boldsymbol{\mu}} \cdot \mathbf{H}$$

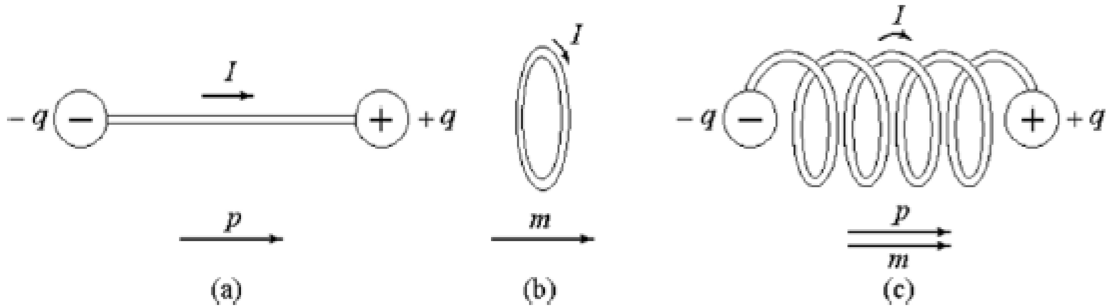

<u>chiral materials</u> $\boxed{\xi = \zeta^*}$ pure imaginary

- **Aligned electric dipoles and magnetic dipoles appear simultaneously under the action of an electric field or a magnetic field alone.**

Literature Review

3D Chiral Structure

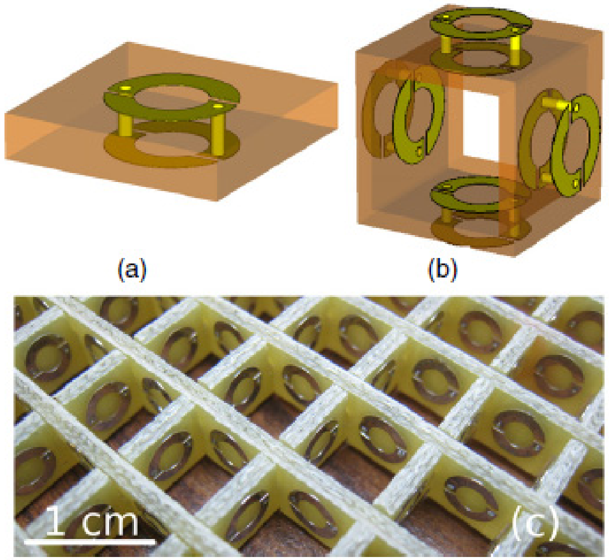

Appl. Phys. Lett. **94** 15 (2009)

Planar Chiral Structure

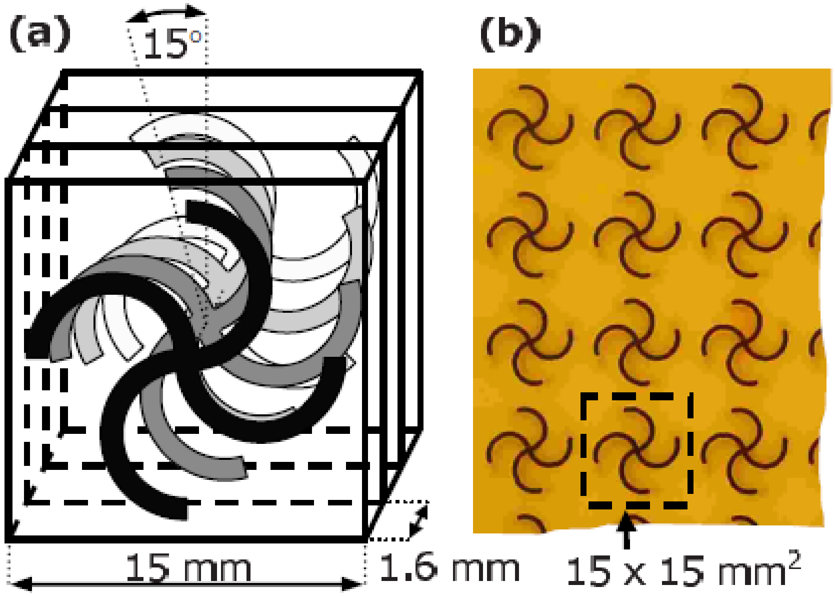

Phys. Rev. B **79**, 3 (2009)

- **Proposed chiral structure**
  - Simple 3D chiral geometry
  - Conveniently fabricated on PCB
  - Great capability to manipulate the polarization state of EM waves
  - Large tunability

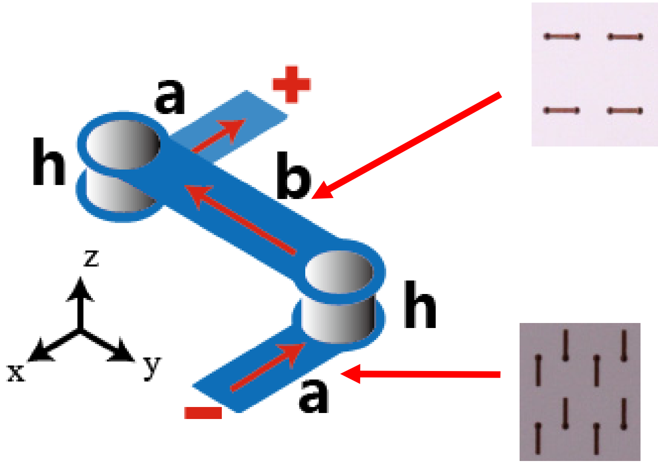

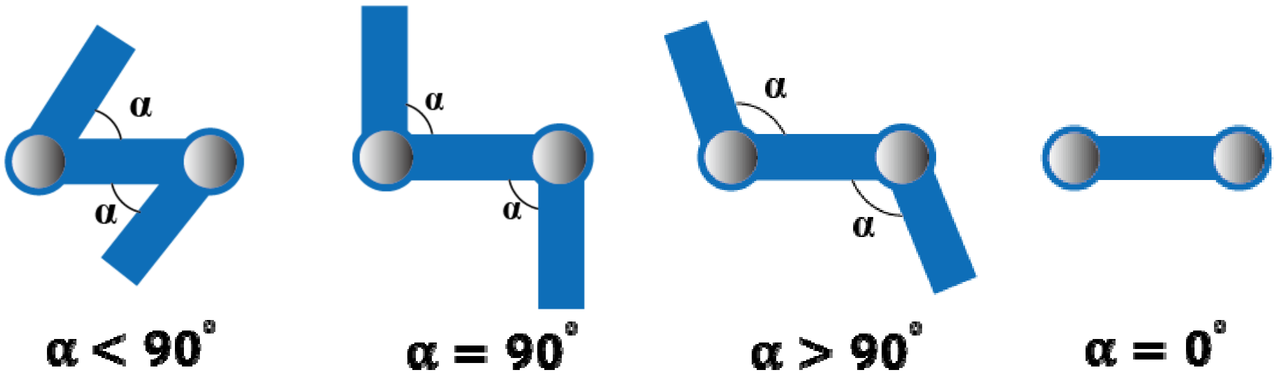

- **<u>Two</u> pairs of <u>aligned</u> ME dipoles**

$l = 2a + b + 2h$

$l = \lambda_{eff}/2$

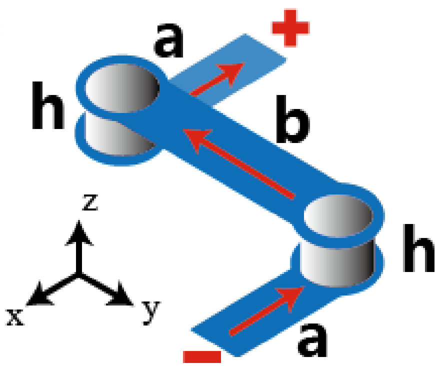

(a) 3D of the chiral particle resonating at the fundamental mode

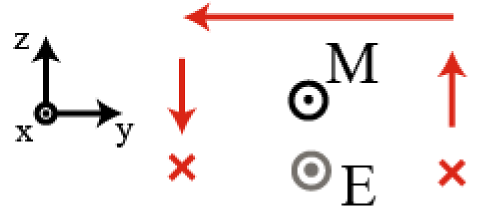

(b) Current distribution viewed from the *x* axis and induced ME dipole pair along the *x* direction

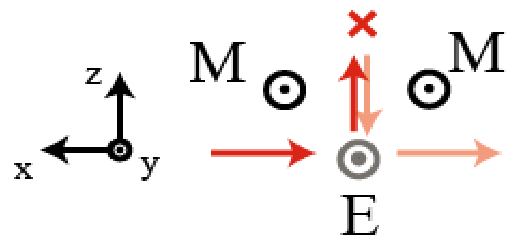

(b) Current distribution viewed from the *y* axis and induced ME dipole pair along the *y* direction

Transmission Matrix

- **Assume a plane wave propagates along the z direction**

$$\mathbf{E}_i(\mathbf{r},t) = \begin{pmatrix} i_x \\ i_y \end{pmatrix} e^{i(kz-\omega t)}, \quad \mathbf{E}_t(\mathbf{r},t) = \begin{pmatrix} t_x \\ t_y \end{pmatrix} e^{i(kz-\omega t)}$$

$i_{x,y}$ and $t_{x,y}$ are polarization states of incident and transmitted waves.

- **Chiral particle modelling**

$$\begin{pmatrix} t_x \\ t_y \end{pmatrix} = \begin{pmatrix} T_{xx} & T_{xy} \\ T_{yx} & T_{yy} \end{pmatrix} \begin{pmatrix} i_x \\ i_y \end{pmatrix} = T_{lin} \begin{pmatrix} i_x \\ i_y \end{pmatrix}$$

Linear basis

$$T_{circ} = \begin{pmatrix} T_{++} & T_{+-} \\ T_{-+} & T_{--} \end{pmatrix} = \frac{1}{2} \begin{pmatrix} (T_{xx}+T_{yy}) + i(T_{xy}-T_{yx}) & (T_{xx}-T_{yy}) - i(T_{xy}+T_{yx}) \\ (T_{xx}-T_{yy}) + i(T_{xy}+T_{yx}) & (T_{xx}+T_{yy}) - i(T_{xy}-T_{yx}) \end{pmatrix}$$

Circular basis

Circular Polarizer Design

- **Convert an *x* polarized wave to a circularly polarized wave**

$$|T_{xx}| = |T_{yx}|,\ \arg(T_{xx}) - \arg(T_{yx}) = \pm 90°$$

- **Special relationship for ±α**

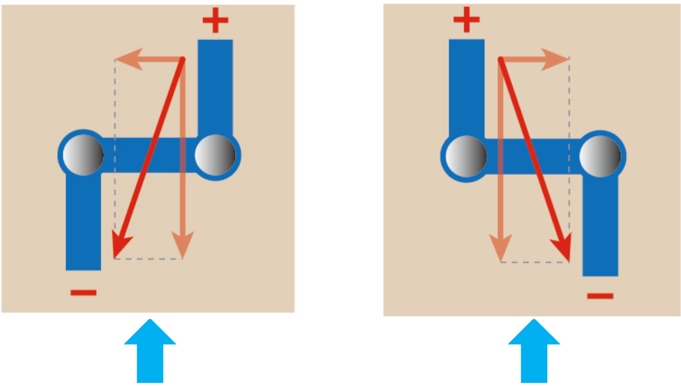

Right-handed circular polarizer

Left-handed circular polarizer

<u>180° phase difference</u> between the cross-polarized component by switching the orientations of the two arms

$$T_{lin}^{\alpha} = \begin{pmatrix} T_{xx} & T_{xy} \\ T_{yx} & T_{yy} \end{pmatrix},\ T_{lin}^{-\alpha} = \begin{pmatrix} T_{xx} & -T_{xy} \\ -T_{yx} & T_{yy} \end{pmatrix}$$

$$\Downarrow$$

$$T_{circ}^{\alpha} = \begin{pmatrix} T_{++} & T_{+-} \\ T_{-+} & T_{--} \end{pmatrix},\ T_{circ}^{-\alpha} = \begin{pmatrix} T_{--} & T_{-+} \\ T_{+-} & T_{++} \end{pmatrix}$$

Experiments

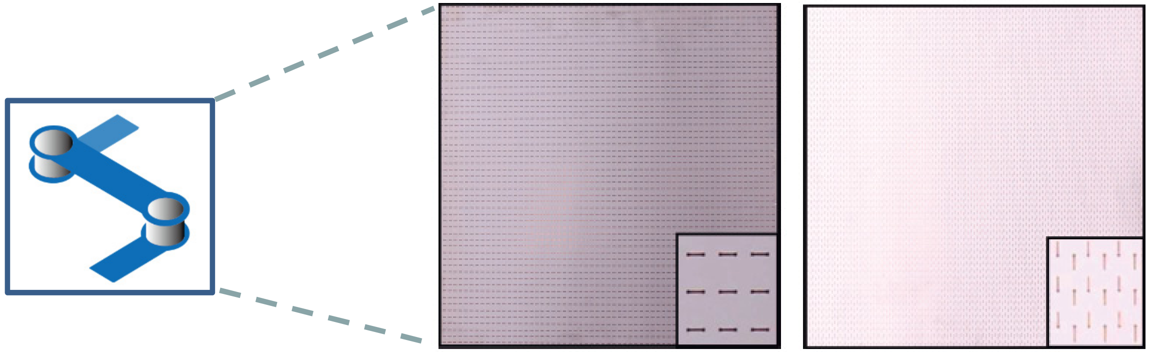

Dielectric substrate: AD600, $\varepsilon_r = 6.15$, h = 1.524 mm

54 × 63 unit cells
378 ×378 mm^2

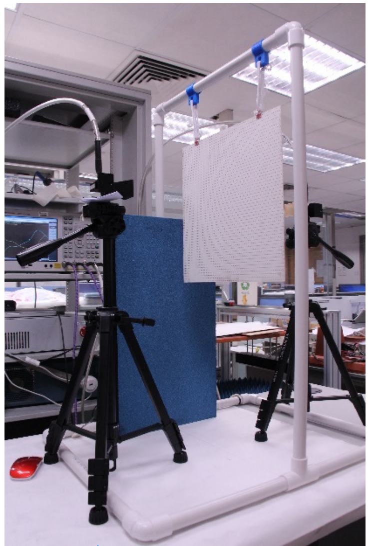

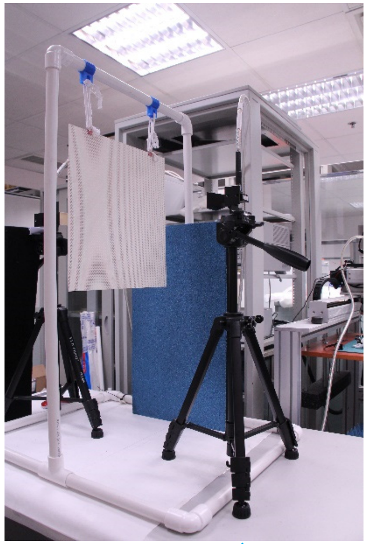

Transmitter

Receiver

Two horn antennas:

- linear polarized
- working frequency: 6.57 GHz ~ 9.99 GHz

Measure

Transmission matrix in linear basis

Calculate

T_{circ}

Results

➢ Simulation and experiment results

- Working frequency 9.2 GHz
- Efficiency 64%
- Compact size: unit cell size of 0.21 $\lambda_0 \times 0.18 \lambda_0$
- Conveniently implementation of both right- and left-handed circular polarizer

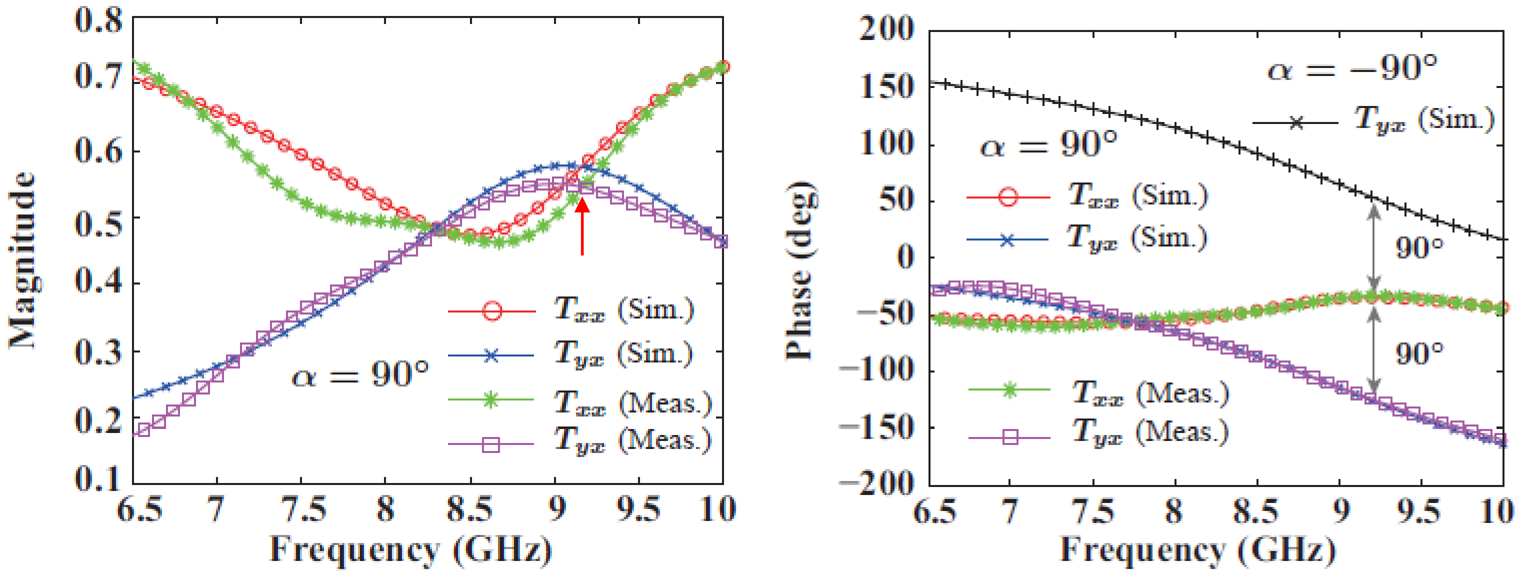

3.2. Orbital Angular Momentum Generation by Metasurfaces

[2] M. L. N. Chen, L. J. Jiang, and W. E. I. Sha, "Artificial perfect electric conductor-perfect magnetic conductor anisotropic metasurface for generating orbital angular momentum of microwave with nearly perfect conversion efficiency," *Journal of Applied Physics*, vol. 119, no. 6, pp. 064506, 2016.

[3] M. L. N. Chen, L. J. Jiang, and W. E. I. Sha, "Unltra-thin complementary metasurface for orbital angular momentum generation at microwave frequencies," *IEEE Trans. Antennas Propag.,* vol. 65, no. 1, pp. 396-400, Jan. 2017.

Literature Review

Spiral Phase Plate

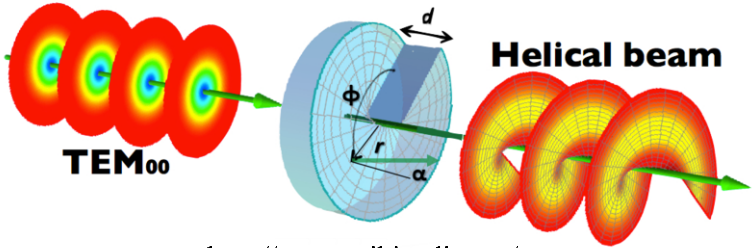

http://www.wikipedia.org/

Travelling-Wave Antenna

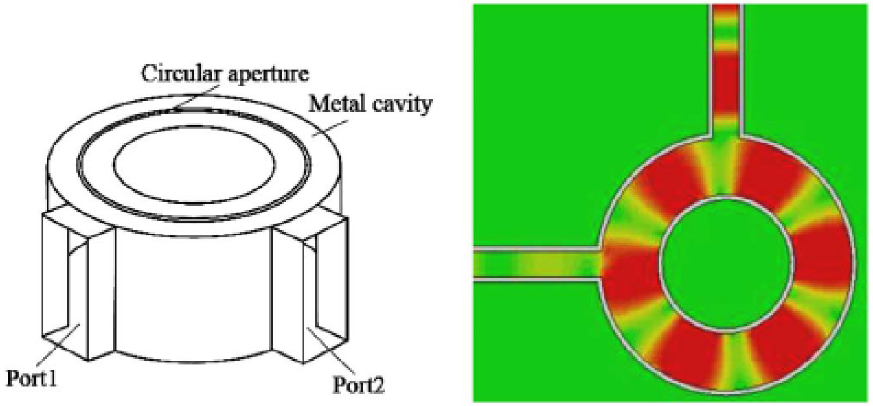

IEEE Trans. Antennas. Propag. **63** 4 (2015)

Metasurface

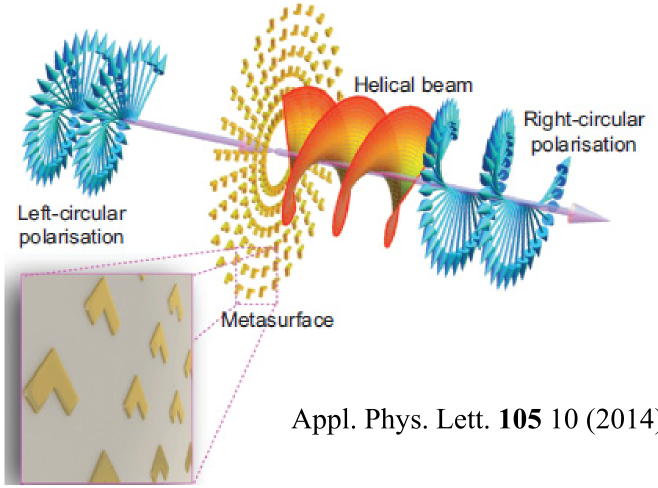

Appl. Phys. Lett. **105** 10 (2014)

Computer Generated Hologram

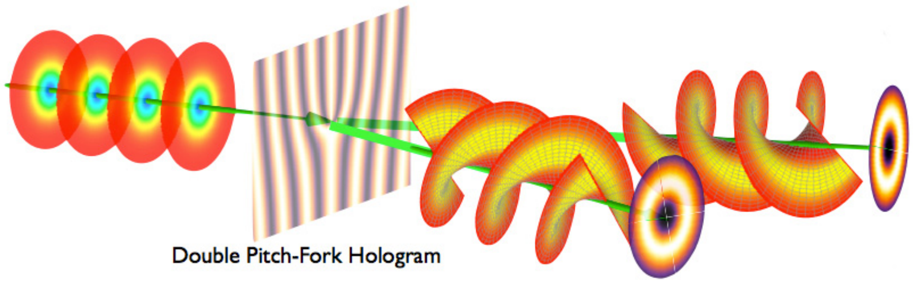

http://www.wikipedia.org/

Challenges at Microwave Regime

- **Efficiency**

  Absorption and reflection of scatterers

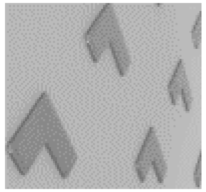

- **Complexity**

  Bulk at microwave based on the scaling law

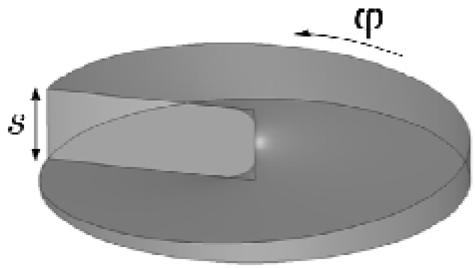

- **Difference between optics and microwave regime**

  components at optics are not easy to be replicated at microwave regime (At optics, we have hologram, beam splitter…)

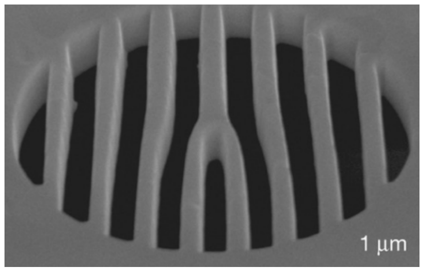

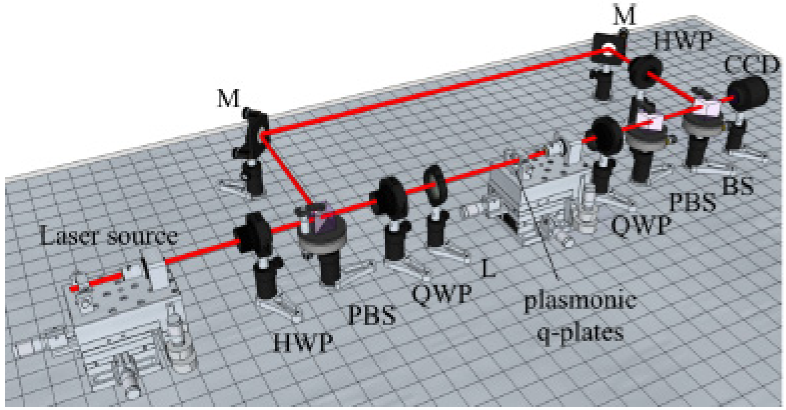

Design Objective

- **Orbital angular momentum generation at microwave regime**
  - Metasurface: <u>low profile, high efficiency</u>
  - Principle: momentum conservation law or berry phase based concept
  - Incident wave: Circularly polarized <u>plane wave</u>
  - Transmitted wave: Cross-circularly polarized <u>vortex wave</u>

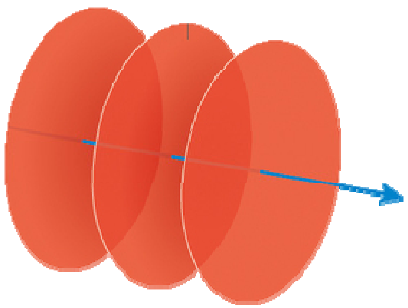

Plane wave:
$\boldsymbol{E}(\boldsymbol{r}, t)$

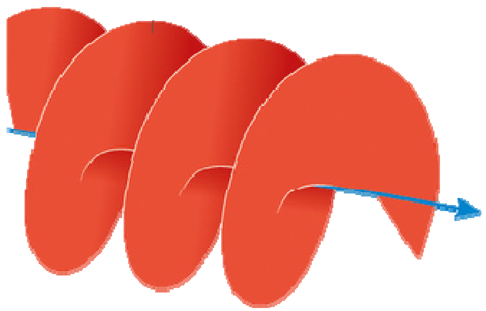

Vortex wave:
$\boldsymbol{E}(\boldsymbol{r}, t)\boldsymbol{e}^{-i\ell\phi}$

Geometric Phase

➢ Scatterer under rotation

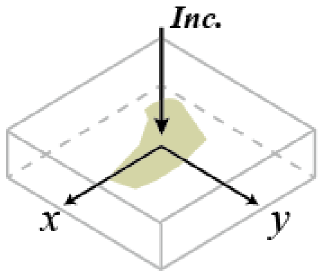

$$\mathbf{J} = \begin{pmatrix} J_{xx} & J_{xy} \\ J_{yx} & J_{yy} \end{pmatrix}$$

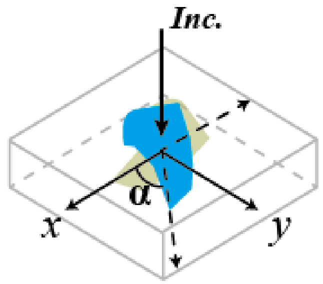

$$\mathbf{J}(\alpha) = \mathbf{R}(-\alpha)\mathbf{J}\mathbf{R}(\alpha)$$

$$\mathbf{R}(\alpha) = \begin{pmatrix} \cos\theta & \sin\theta \\ -\sin\theta & \cos\theta \end{pmatrix}$$

➢ Scatterer that shifts the circular polarization state

- $J_{xx} = -J_{yy}$ & $J_{xy} = J_{yx} = 0$

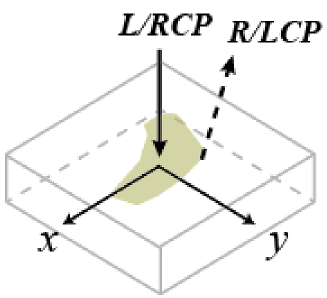

$$\mathbf{J} = \begin{pmatrix} J_{xx} & 0 \\ 0 & -J_{xx} \end{pmatrix}$$

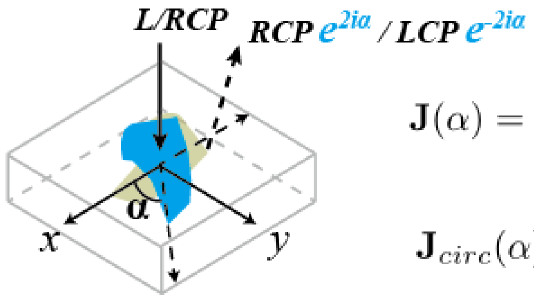

$$\mathbf{J}(\alpha) = J_{xx} \begin{pmatrix} \cos(2\alpha) & \sin(2\alpha) \\ \sin(2\alpha) & -\cos(2\alpha) \end{pmatrix}$$

$$\mathbf{J}_{circ}(\alpha) = J_{xx} \begin{pmatrix} 0 & e^{-2i\alpha} \\ e^{2i\alpha} & 0 \end{pmatrix}$$

geometric phase

Geometric Phase vs Azimuthal Phase Dependence

➢ **Geometric phase is modulated to coincide with the azimuthal phase dependence factor**

Geometric phase $e^{-2i\alpha}$ ⟶ Phase factor for OAM $e^{-il\varphi}$

- Rotation angle α is determined by OAM order $\underline{\alpha = l\,\varphi / 2}$
- Scatterers with spatially varying rotation angle α according to their azimuthal location angle φ

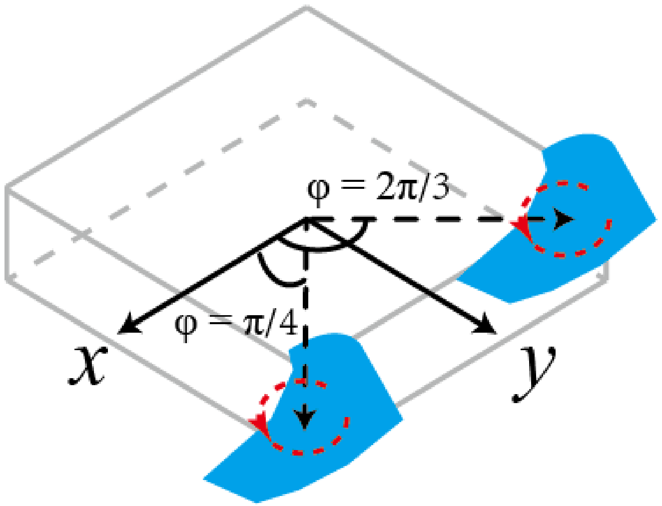

$$e^{-il\,2\pi/3} \begin{cases} l = 1,\ \alpha = \pi/3 \\ l = 2,\ \alpha = 2\pi/3 \\ l = 3,\ \alpha = 3\pi/3 \\ \quad \cdots \end{cases}$$

$$e^{-il\,\pi/4} \begin{cases} l = 1,\ \alpha = \pi/8 \\ l = 2,\ \alpha = 2\pi/8 \\ l = 3,\ \alpha = 3\pi/8 \\ \quad \cdots \end{cases}$$

Reflective Metasurface

- **Scatterer that shifts the circular polarization state**
  - For x polarized wave, PEC (perfect electric conductor) J_{xx} = -1
  - For y polarized wave, PMC (perfect magnetic conductor) J_{yy} = 1

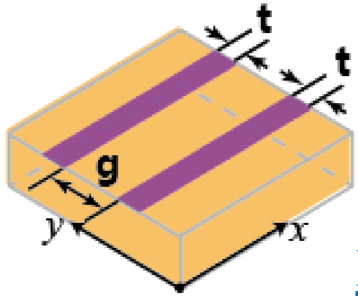

PEC

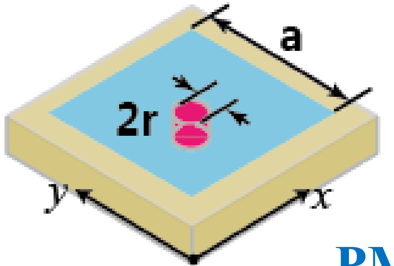

PMC

- **Parallel-plate waveguide**
  - Dimensions are designed so that the working frequency is below the cutoff TE frequency
- **Mushroom-type high impedance surface**
  - Resonance at working frequency

Scatterer Design

➢ **Simulated reflection coefficients of a single scatterer**

- Amplitudes of the <u>co-polarized reflection coefficients</u> are 1
- Reflection phase by the strip array is <u>constant and 180°</u>
- Reflection phase by the mushroom varies and is <u>zero at the resonance</u>

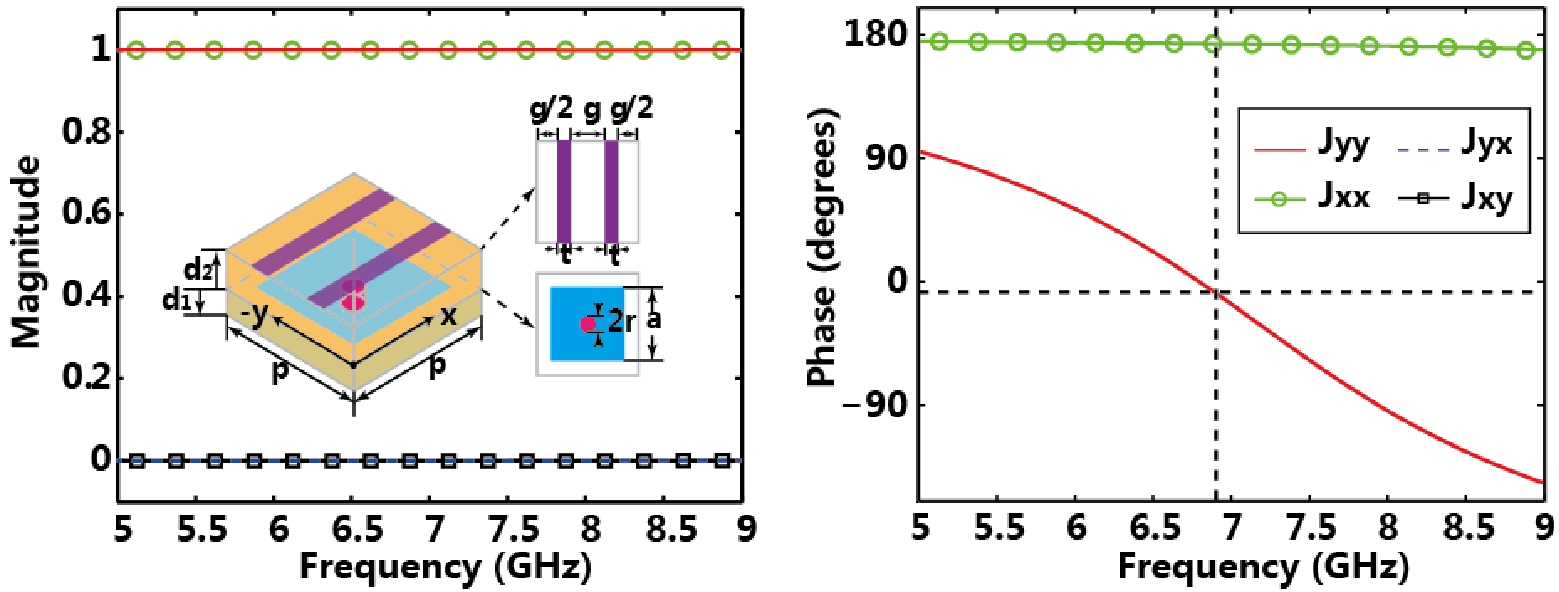

Dielectric substrate: $\varepsilon_r = 2.2$, $d_1 = 2$ mm, $d_2 = 3$ mm
Geometric parameters: p = 7 mm; t = 1 mm, g = 2.5 mm; a = 6 mm, r = 0.25 mm

Metasurface Design

- **Schematic pattern of the continuous PEC-PMC metasurface**
  - Order of OAM $\underline{l = 2\alpha / \varphi = 2}$
  - PEC surface, a series of concentric loops
  - PMC surface, isotropic, no need to rotate

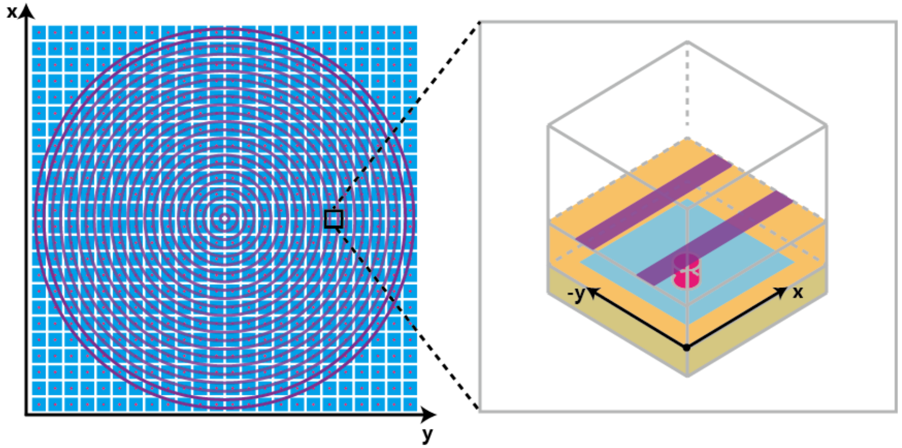

- **Simulated field patterns at a transverse plane of $z = 0.4\ \lambda_0$**
  - Right-circularly polarized incidence

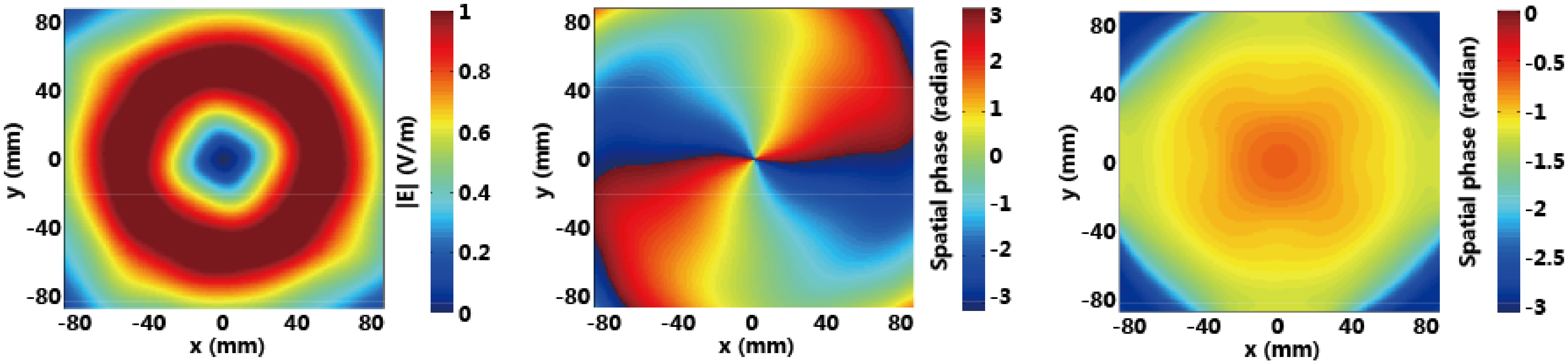

(a) Amplitude of the reflected *E* field (b) Phase of the reflected *E* field (c) Phase of the incident *E* field

Arbitrary-Order OAM Generation

➢ **To generate OAM with <u>arbitrary orders</u>**

- Replace the PEC layer by <u>dipole scatterers</u>
- Keep the PMC layer unchanged
- At the <u>half-wavelength</u> resonance of dipole, the reflection phase is 180°
- Amplitudes of the co-polarized reflection coefficients are 1

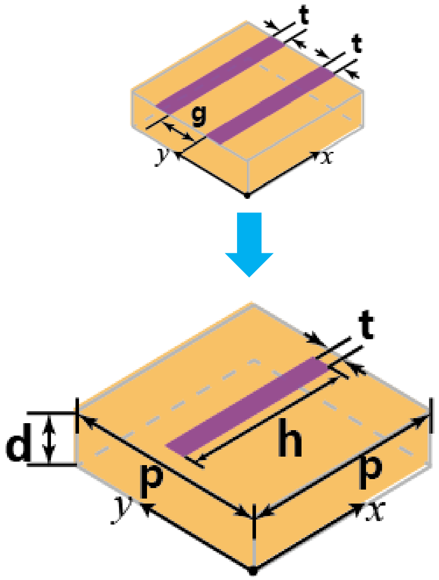

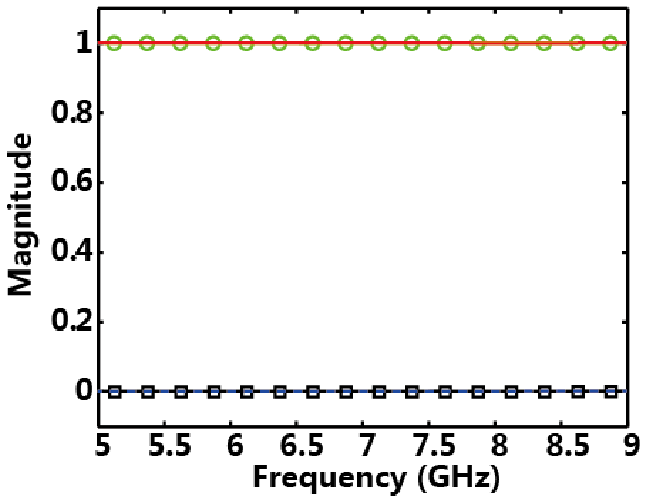

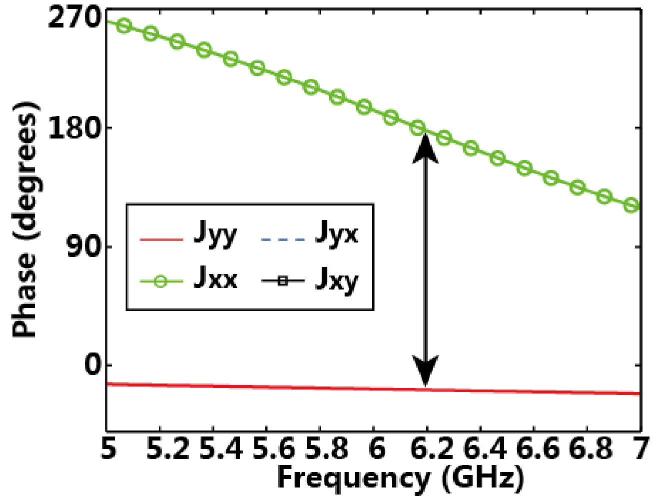

Geometric parameters: h = 23 mm, t = 4 mm; p = 27 mm; d = 1 mm

Simulation Results

- ❑ **Field patterns at a transverse plane of $z = 0.8\ \lambda_0$**

OAM of order 2

OAM of order 4

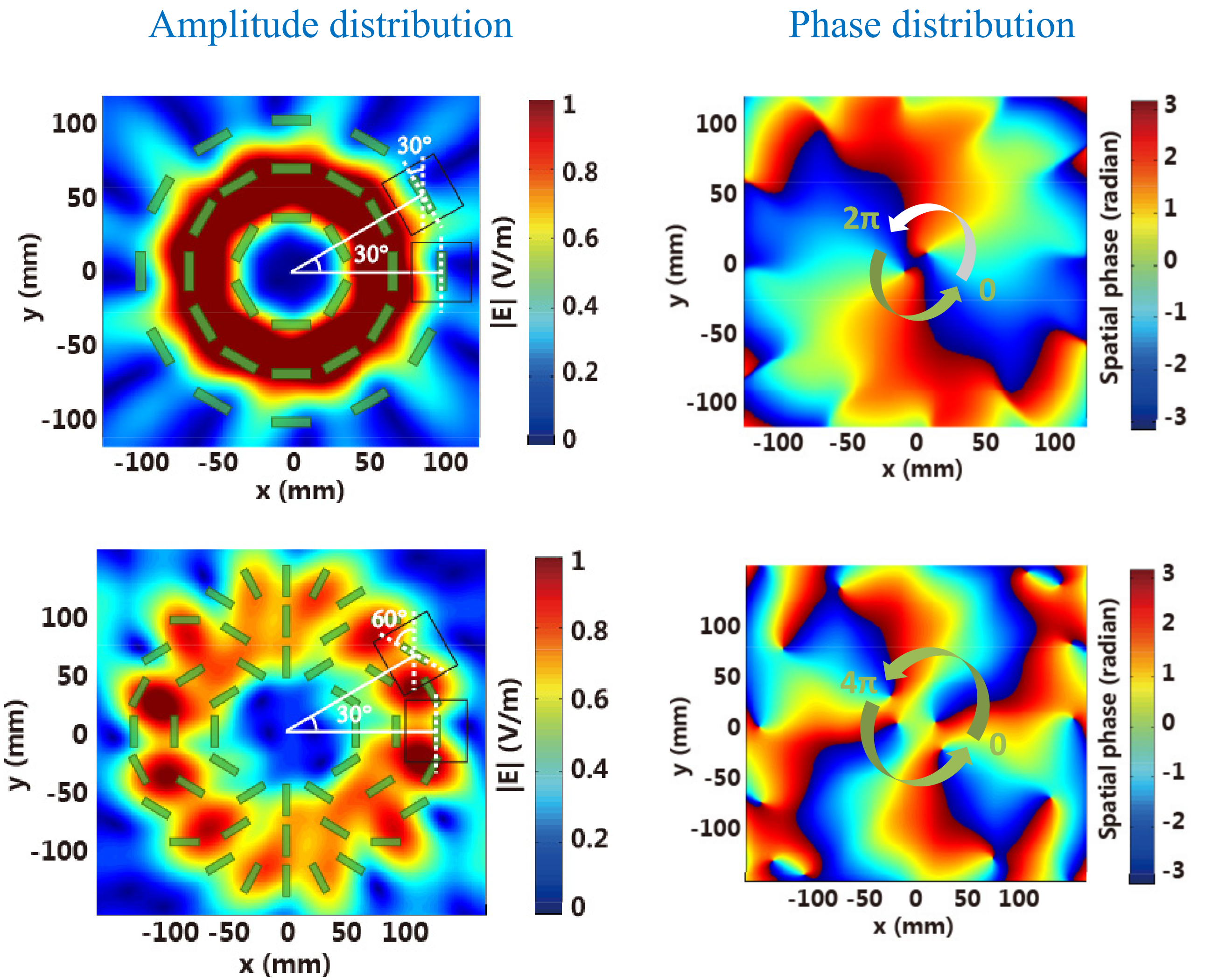

Transmittive Metasurface

- **Objective**

• $\mathbf{J} = \begin{pmatrix} J_{xx} & J_{xy} \\ J_{yx} & J_{yy} \end{pmatrix} \longrightarrow \mathbf{T} = \begin{pmatrix} T_{xx} & T_{xy} \\ T_{yx} & T_{yy} \end{pmatrix}$ $T_{xx} = -T_{yy}$ & $T_{xy} = T_{yx} = 0$

- **Bi-layer complementary split ring resonators (CSRRs) by Babinet Principle**

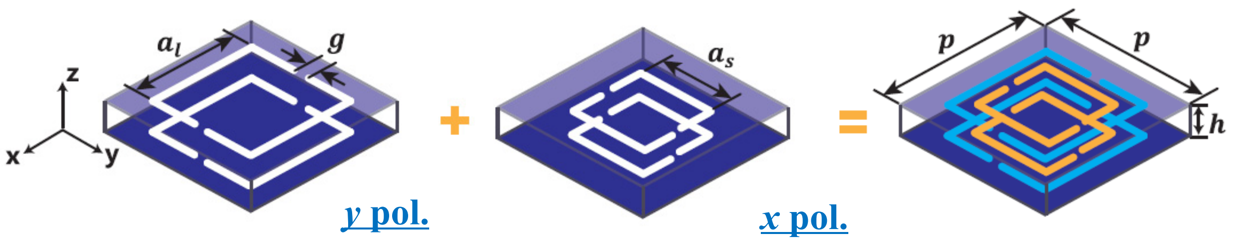

- **Equivalent circuit model**

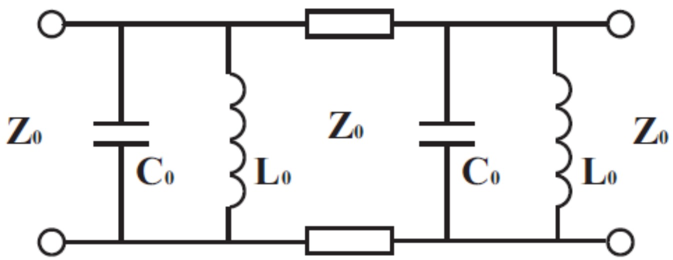

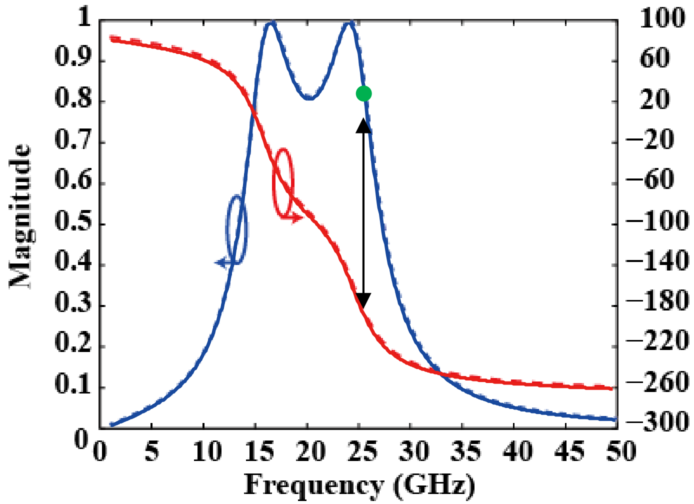

Simulation Results by CST

➢ **Simulated transmission coefficients of the proposed scatterer**

@ Designed frequency (17.85 GHz)

- Magnitudes of T_{xx} and T_{yy} are 0.91 (almost 1)
- Their phase difference is 180°
- 81% conversion efficiency

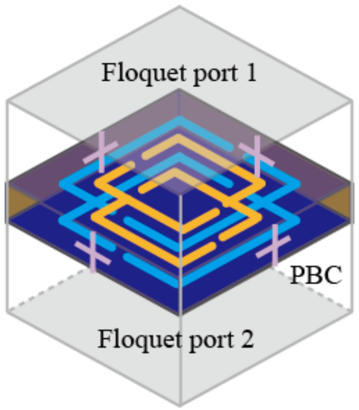

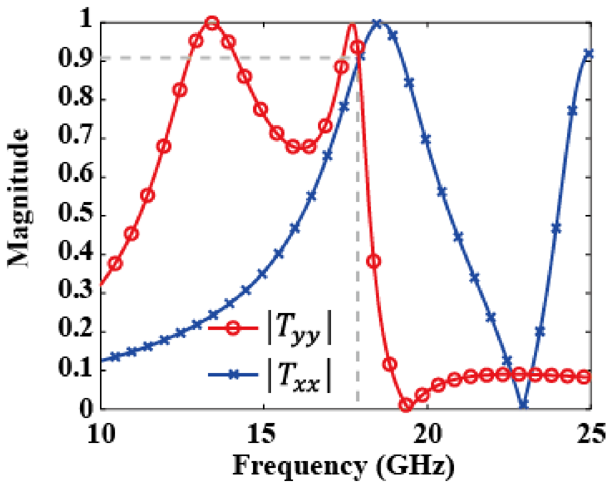

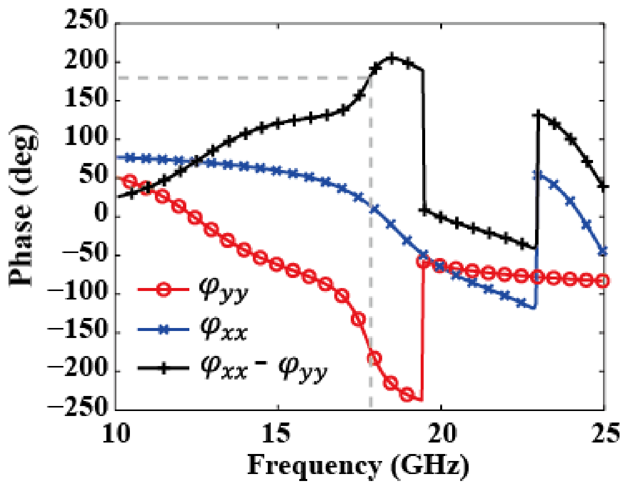

Dielectric substrate: F4B220, $\varepsilon_r = 2.2$, h = 0.8 mm

Geometric parameters: The period of the unit cell is 7×7 mm^2. Side lengths of the two types of square CSRRs are a_l = 5.2 mm and a_s = 3.9 mm. The length of the complementary gap is g = 0.2 mm. The width of the slots is t = 0.2 mm.

Metasurface Design

➢ Geometry of the metasurfaces (top view)

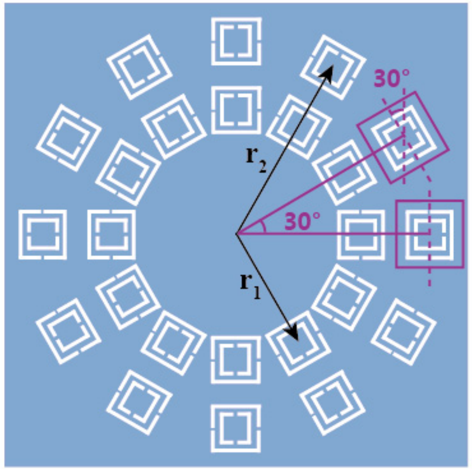

OAM of order $l = 2\alpha/\varphi = 2$

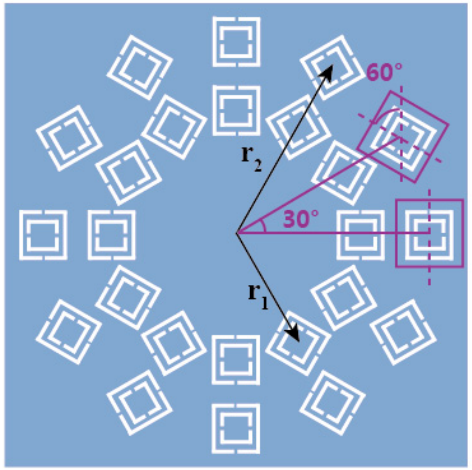

OAM of order $l = 2\alpha/\varphi = 4$

➢ Simulation approaches

- Equivalent magnetic dipoles
- Simulation software

Numerical Simulation

➢ Magnetic dipole approximation

- Equivalent magnetic point source by equivalence principle
- Green’s function

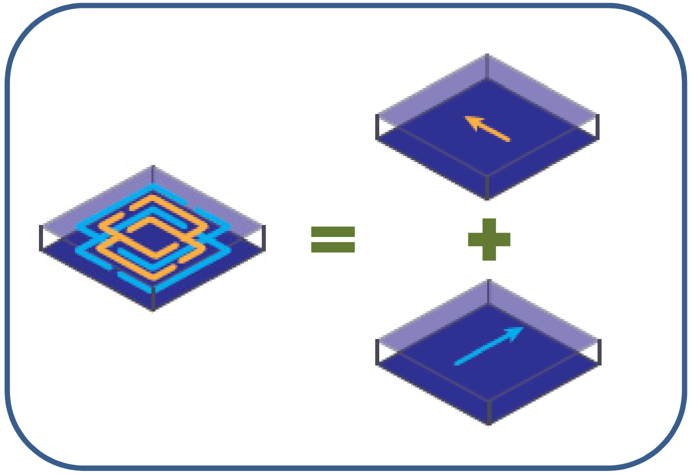

$$\mathbf{E}(\mathbf{r}) = 2\int_V \overline{\mathbf{G}}_m(\mathbf{r},\mathbf{r}')\cdot\mathbf{M}(\mathbf{r}')d\mathbf{r}' = 2\int_V \nabla g(\mathbf{r},\mathbf{r}')\times\mathbf{M}(\mathbf{r}')d\mathbf{r}'$$

Numerical Results

- Approximate field patterns at a transverse plane of $z = 0.6\ \lambda_0$

Amplitude distribution | Phase distribution

OAM of order 2

OAM of order 4

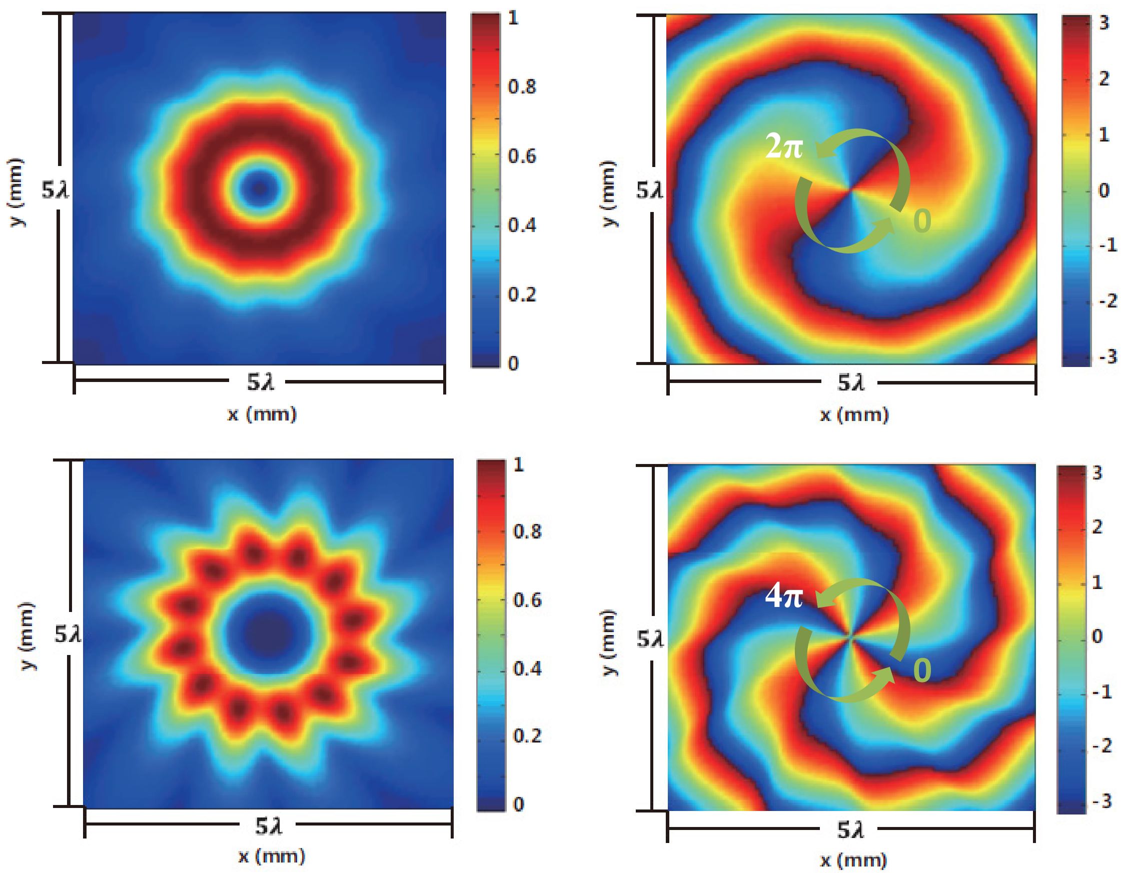

Full-Wave Simulation Results

❑ **Full-wave simulated field patterns at a transverse plane of $z = 0.6\ \lambda_0$**

Amplitude distribution | Phase distribution

OAM of order 2

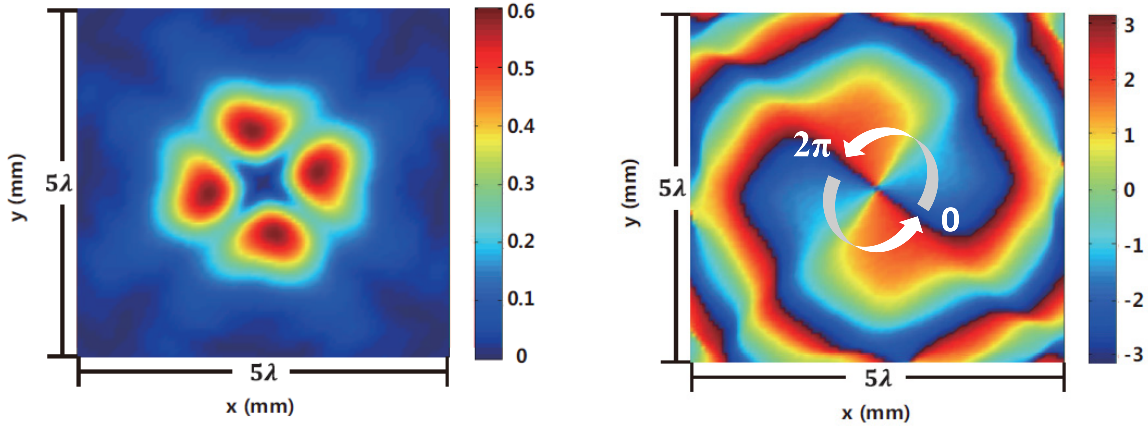

OAM of order 4

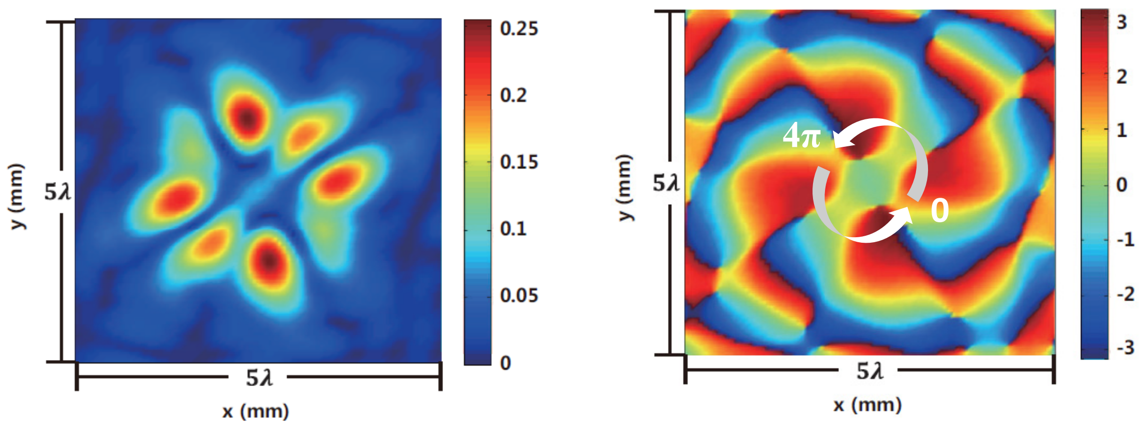

4. Spin and Orbital Angular Momenta Mixing

[1] X. Y. Z. Xiong, A. A.-Jarro, L. J. Jiang, N. C. Panoiu, and W. E. I. Sha, "Mixing of Spin and Orbital Angular Momenta via Second-Harmonic Generation in Plasmonic and Dielectric Chiral Nanostructures," Phys. Rev. B, vol. 95, no. 16, pp. 165432, Apr. 2017.

[2] M. Fang, Z. X. Huang, W. E. I. Sha, X. Y. Z. Xiong, and X. L. Wu, "Full Hydrodynamic Model of Nonlinear Electromagnetic Response in Metallic Metamaterials (invited paper)," PIER, vol. 157, pp. 63-78, Oct. 2016.

Near-field Distribution

- Radius of the gold sphere: 100 nm
- Wavelength of the incident beam: 520 nm
- Near-field observation plane: 40 nm away from the back side of the sphere
- Laguerre-Gaussian (LG) beam with OAM $l = 1$, SAM $\sigma = +1/-1$.

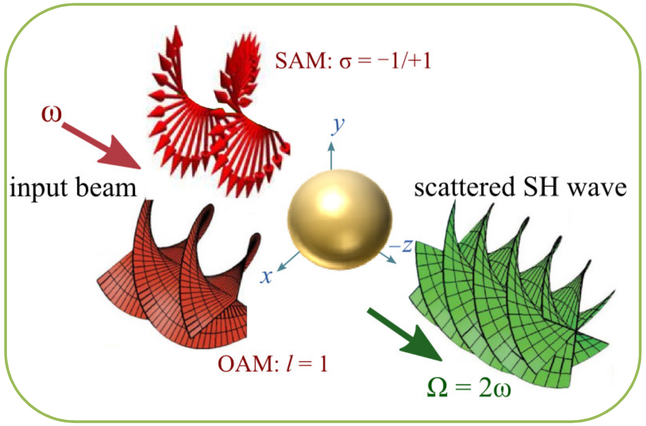

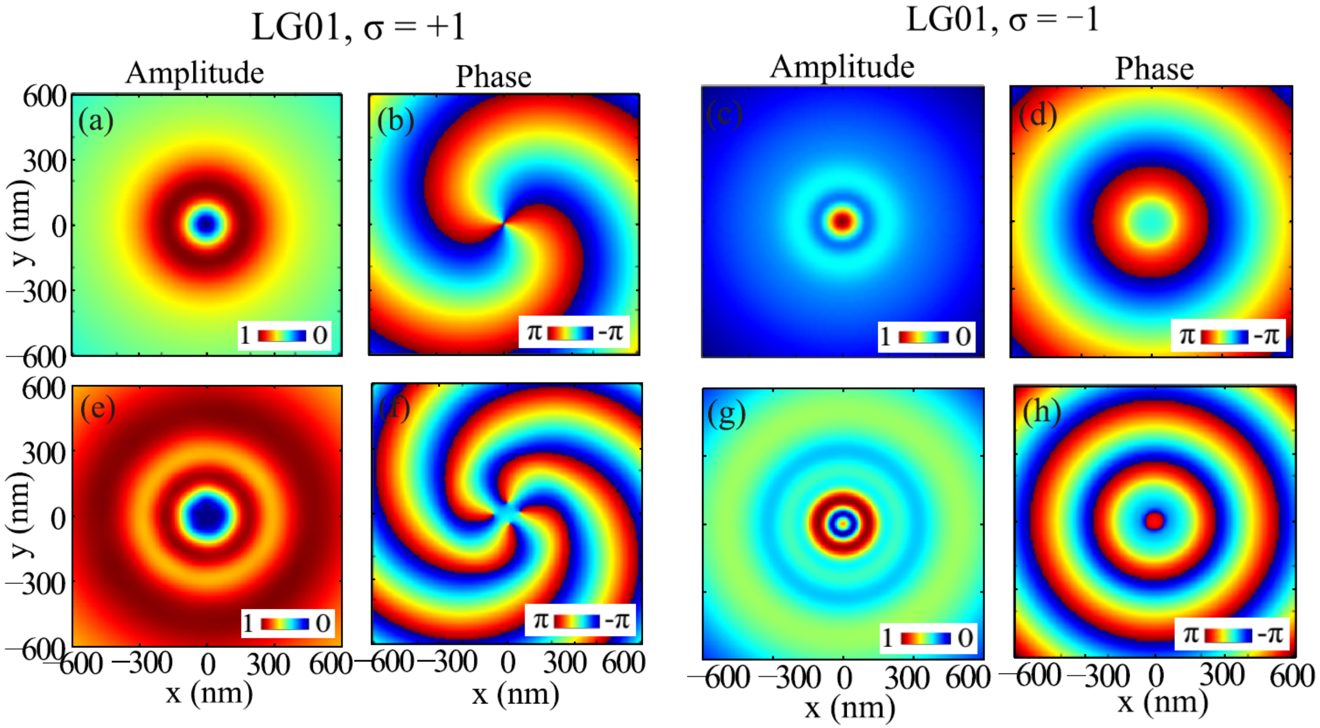

Fundamental

Second-Harmonic (SH)

A Single Silicon Nanosphere

Scattering Cross Section (SCS) Analysis

- Radius of the silicon sphere: 500 nm
- Laguerre-Gaussian (LG) beam with OAM $l = 4$, SAM $\sigma = +1/-1$.

Fundamental SCS, linearly polarized plane wave

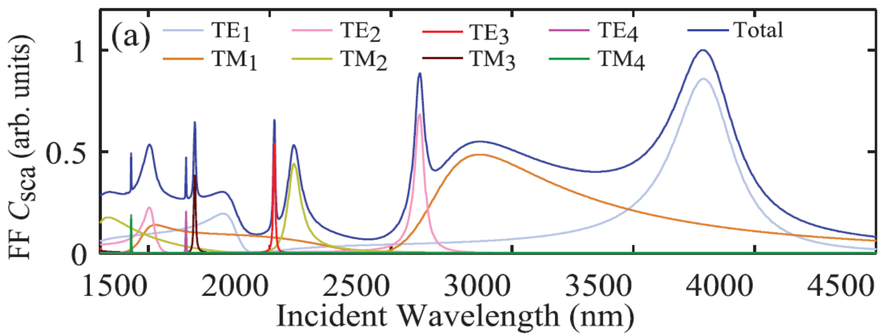

SH SCS, Laguerre-Gaussian beam

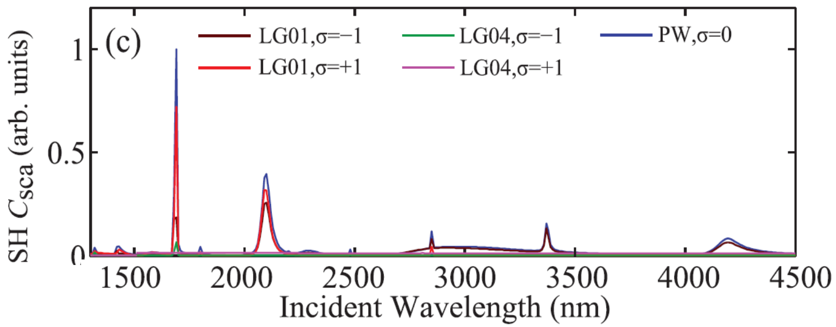

Fundamental SCS, Laguerre-Gaussian beam

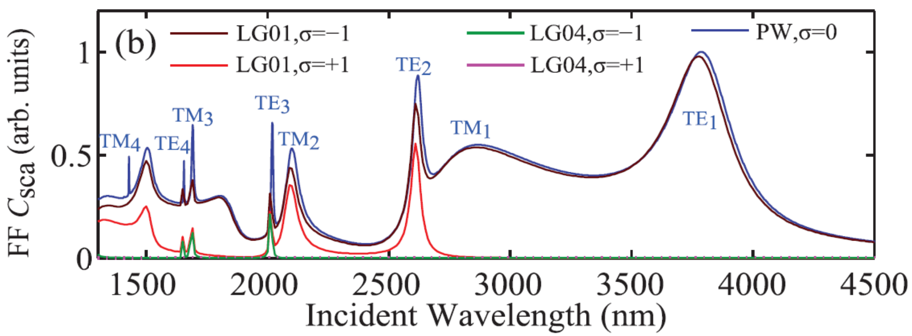

Two SH enhancement mechanisms

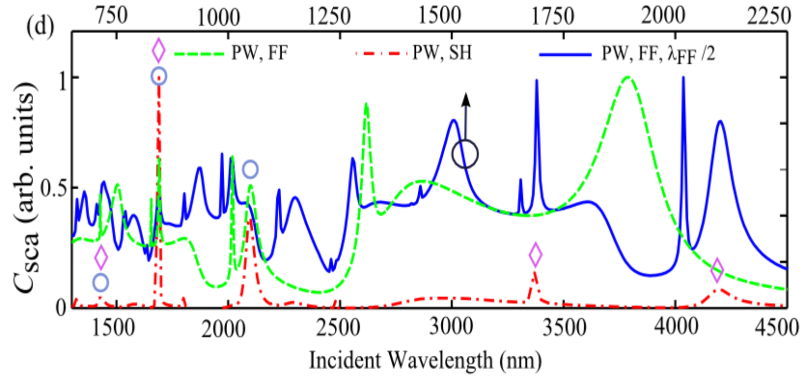

Circles: fundamental mode enhancement; Diamonds: SH induced fundamental mode enhancement

Total Angular Momentum Matching

- Chiral cluster with 3-fold rotational symmetry containing 10 identical silicon nanospheres (*quasi-angular-momentum* $N = 3$)
- Radius of the silicon sphere/cross section: 500 nm
- Laguerre-Gaussian (LG) beam with OAM $l = 4$, SAM $\sigma = +1/-1$.
- Total angular momentum $j = l + \sigma$

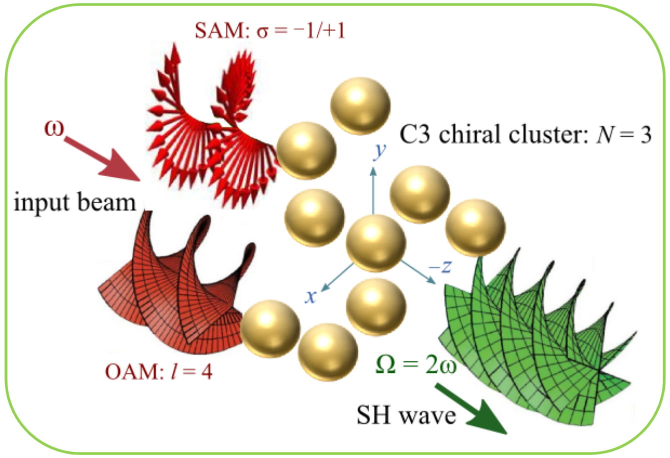

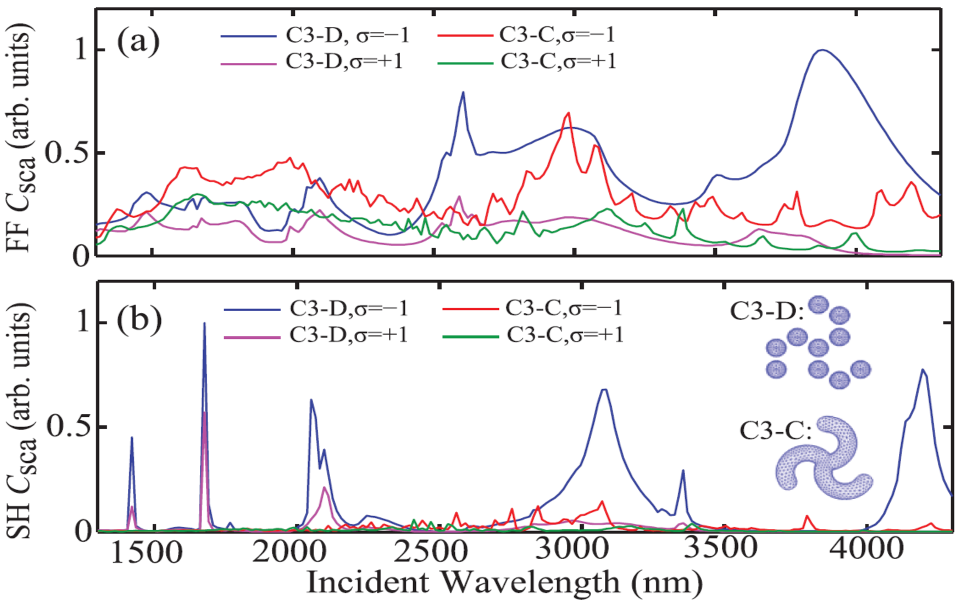

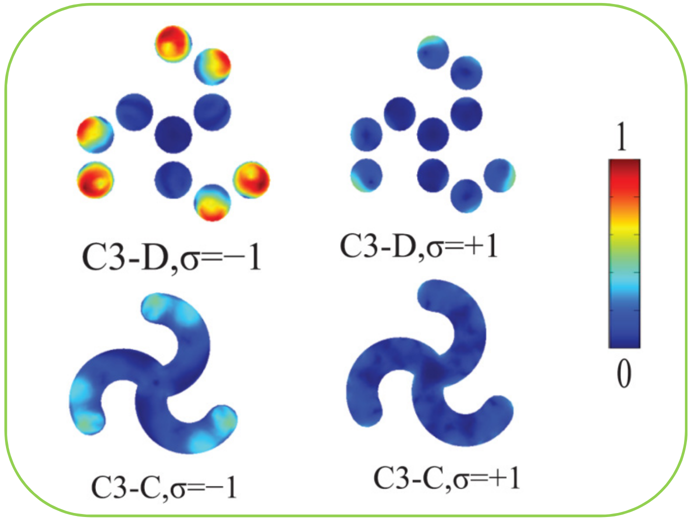

second-harmonic field

Angular Momentum Conservation (1)

General Angular Momentum Conservation Law

- For a naostructure with *N*-fold rotational symmetry

The relation between the spin and orbital angular momenta of the incident field and that of the scattered second-harmonic wave is given by

$$\boxed{j_{sca} = s(l + \sigma) + qN}$$

analogy $\longrightarrow$ translational momentum conservation

$$k_0 \sin\theta_s = s k_0 \sin\theta_i + m\frac{2\pi}{\Lambda}$$

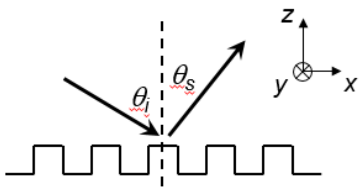

j_{sca}: total angular momentum of the scattered SH wave

σ: spin angular momenta of the incident field ($\sigma = +1$ or $\sigma = -1$)

l: orbital angular momentum of the incident field

s: order of harmonic generation (s = 1 for linear processes, s = 2 for SH generation)

N: quasi-angular-momentum of the nanostructure with N-fold rotational symmetry

q: an integer and $q = 0, \pm 1, \pm 2, \ldots$

Angular Momentum Conservation (2)

experimental [1]

numerical

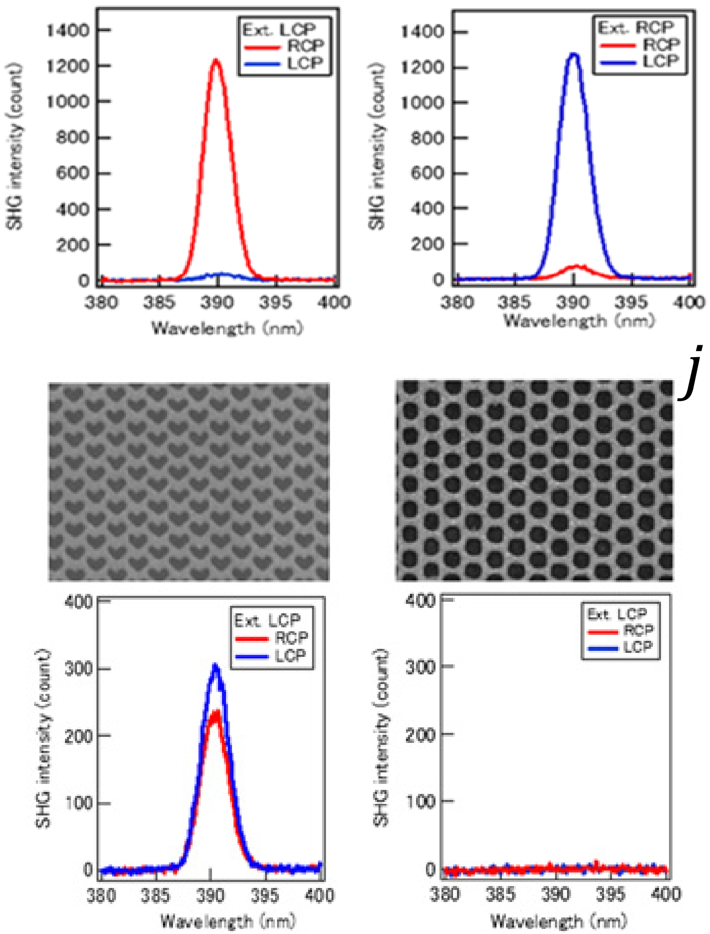

$$j = 2\sigma + qN$$

SH field

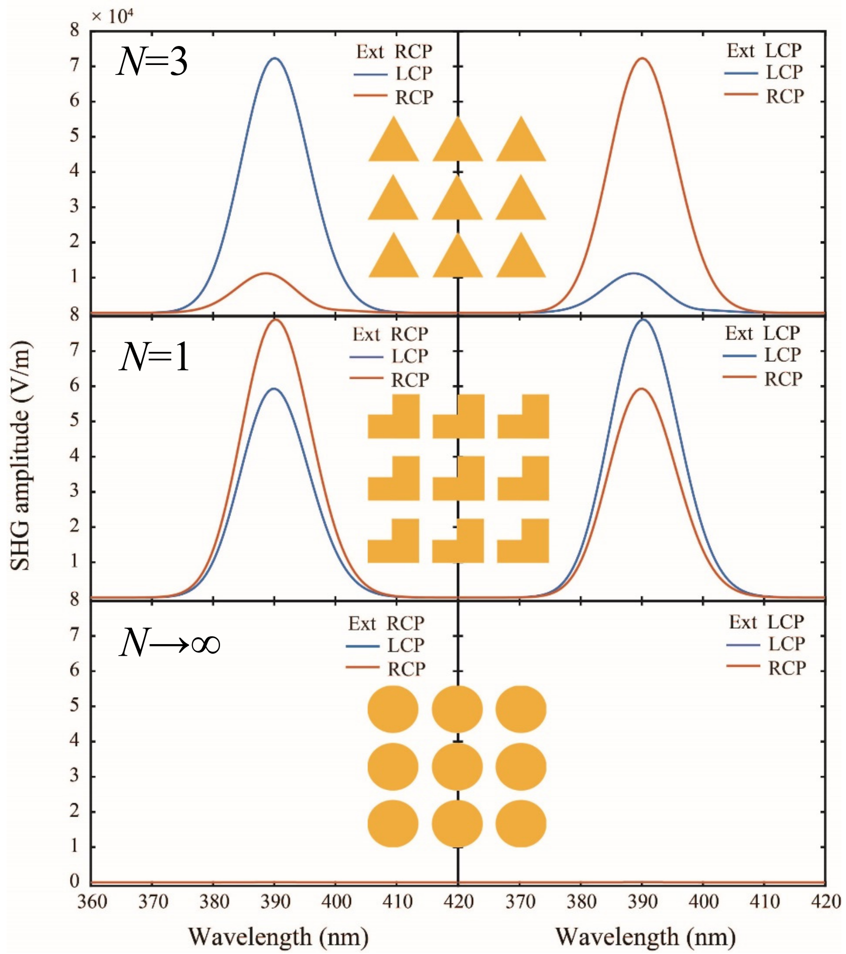

[1] K. Konishi, T. Higuchi, J. Li, J. Larsson, S. Ishii, and M. K.-Gonokami, *Phy. Rev. Lett.* **112**: 135502, 2014.

Angular Momentum Conservation (3)

Angular Momentum Analysis of Nanosphere Cluster by Multipole Expansion

$\sigma = +1, l = 4, N = 3$

FH: $j_{sca} = (l+\sigma) + qN$

SH: $j_{sca} = 2(l+\sigma) + qN$

$j_{sca} = \cdots, -7, -4, -1, 2, 5, 8, \ldots$

$j_{sca} = \cdots, -8, -5, -2, 1, 4, 7, 10, \ldots,$

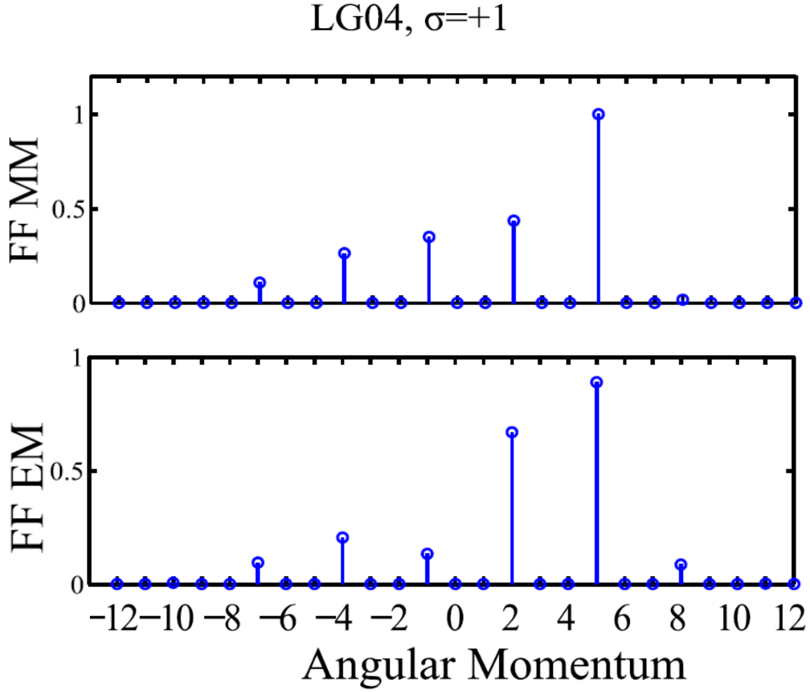

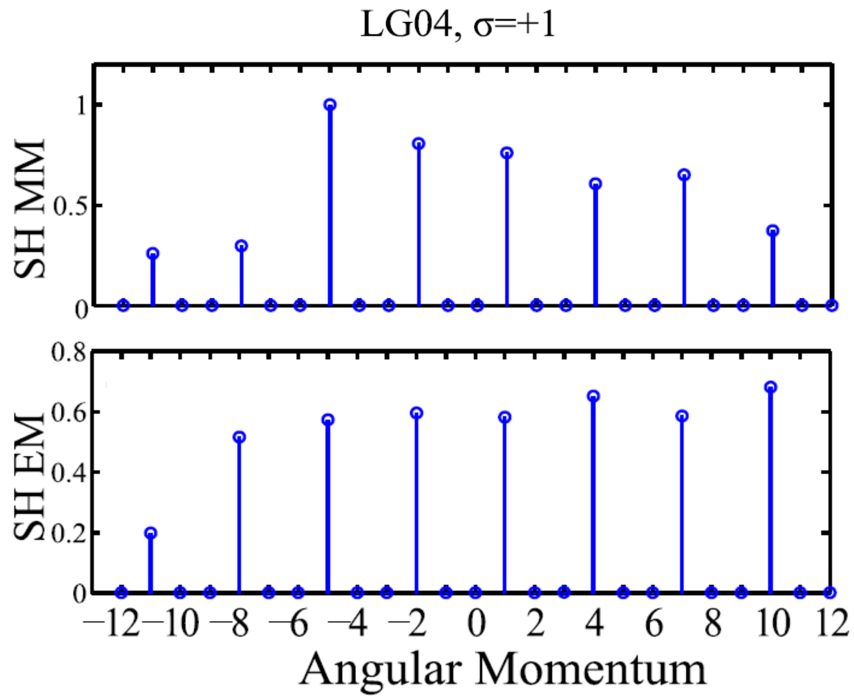

Collaborators

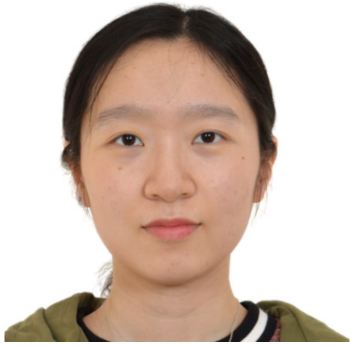

Menglin Chen
(HKU)

Xiaoyan Xiong
(HKU)

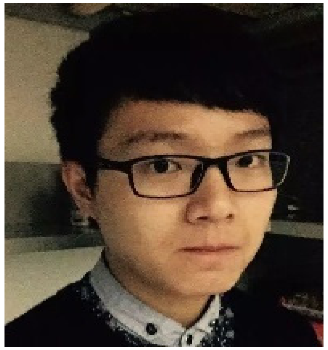

Ming Fang
(AHU)

Ahmed Al-Jarro
(UCL)

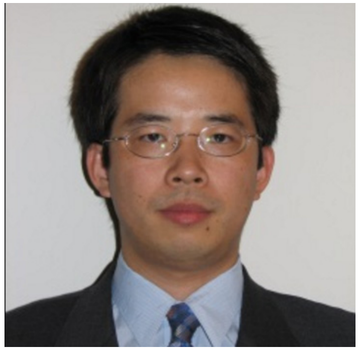

Li Jun Jiang
(HKU)

Weng Cho Chew
(Purdue & HKU)

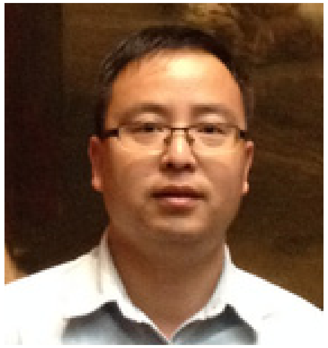

Zhixiang Huang
(AHU)

Nicolae Panoiu
(UCL)

Thanks for your attention!